J. Fluid Mech. (1997), *vol.* 332, *pp.* 263–293

Gradient and counter-gradient scalar transport in turbulent premixed flames

By D. VEYNANTE[1], A. TROUVÉ[2], K. N. C. BRAY[3] AND T. MANTEL[4] †

[1]Laboratoire EM2C, CNRS and Ecole Centrale Paris, 92295 Châtenay-Malabry cedex, France

[2]Institut Français du Pétrole, BP 311, 92506 Rueil-Malmaison cedex, France

[3]Cambridge University, Department of Engineering, Trumpington Street, Cambridge CB2 1PZ, UK

[4]Center for Turbulence Research, Stanford University - NASA-Ames, Bldg. 500 Stanford, CA 94305-3030, USA

(Received 19 July 1995 and in revised form 2 August 1996)

In premixed turbulent combustion, the modelling of the turbulent flux of the mean reaction progress variable $\widetilde{c}$, $\overline{\rho u_i'' c''}$, remains somewhat controversial. Classical gradient transport assumptions based on the eddy viscosity concept are often used while both experimental data and theoretical analysis have pointed out the existence of counter-gradient turbulent diffusion. Direct numerical simulation (DNS) is used in this paper to provide basic information on the turbulent flux of $\widetilde{c}$ and study the occurrence of counter-gradient transport. The numerical configuration corresponds to two- or three-dimensional premixed flames in isotropic turbulent flow. The simulations correspond to various flame and flow conditions that are representative of flamelet combustion. They reveal that different flames will feature different turbulent transport properties and that these differences can be related to basic dynamical differences in the flame–flow interactions: counter-gradient diffusion occurs when the flow field near the flame is dominated by thermal dilatation due to chemical reaction, whereas gradient diffusion occurs when the flow field near the flame is dominated by the turbulent motions. The DNS-based analysis leads to a simple expression to describe the turbulent flux of $\widetilde{c}$, which in turn leads to a simple criterion to delineate between the gradient and counter-gradient turbulent diffusion regimes. This criterion suggests that the occurrence of one regime or the other is determined primarily by the ratio of turbulence intensity divided by the laminar flame speed, u'/s_L, and by the flame heat release factor, $\tau \equiv (T_b - T_u)/T_u$, where T_u and T_b are respectively the temperature within unburnt and burnt gas. Consistent with the Bray–Moss–Libby theory, counter-gradient (gradient) diffusion is promoted by low (high) values of u'/s_L and high (low) values of τ. DNS also shows that these results are not restricted to the turbulent transport of $\widetilde{c}$. Similar results are found for the turbulent transport of flame surface density, Σ. The turbulent fluxes of $\widetilde{c}$ and Σ are strongly correlated in the simulated flames and counter-gradient (gradient) diffusion of $\widetilde{c}$ always coincides with counter-gradient (gradient) diffusion of Σ.

---

† Present address: Renault, Direction de la Recherche, 9–11 Av. du 18 Juin 1940, 92500 Rueil-Malmaison, France.

1. Introduction

The objective of theoretical descriptions of turbulent reacting flows is to provide tractable expressions for unclosed terms appearing in the mean conservation equations for mass, momentum and energy. In the classical theory of turbulent premixed flames, using the assumption of single-step chemistry and unity Lewis number (i.e. identical mass and thermal diffusivities), the mass fractions of the reactive species and the temperature are all linearly related and may be expressed in terms of a single reduced mass fraction called the reaction progress variable, $c \equiv (Y_{R,u} - Y_R)/(Y_{R,u} - Y_{R,b})$, where Y_R is the fuel mass fraction and $Y_{R,u}$ ($Y_{R,b}$) its value in the unburnt (burnt) gas; $c = 0$ within fresh reactants and $c = 1$ within burnt products. Using the classical Favre decomposition, each quantity q can be split into a mass-weighted mean, $\widetilde{q} \equiv \overline{\rho q}/\overline{\rho}$, and a turbulent fluctuation, q''; the transport equation for the mean reaction progress variable $\widetilde{c}$ may then be written as

$$\frac{\partial \overline{\rho}\widetilde{c}}{\partial t} + \frac{\partial \overline{\rho}\widetilde{u}_i\widetilde{c}}{\partial x_i} + \frac{\partial \overline{\rho u_i'' c''}}{\partial x_i} = \overline{\frac{\partial \mathscr{J}_k}{\partial x_k}} + \overline{\omega}_c, \tag{1.1}$$

where ρ is the mass density; u_i is the flow velocity; $\mathscr{J}_k$ is the molecular diffusion flux of c; $\dot{\omega}_c$ is the mass of product produced by the chemical reaction, per unit time and per unit volume; and the overbar denotes conventional ensemble averaging. Equation (1.1) has the form of a standard turbulent transport equation where the rate of change of $\widetilde{c}$ results from a balance between convection by the mean flow, convection by the turbulent flow, molecular diffusion, and chemical reaction. The contribution of molecular diffusion is usually neglected for high Reynolds number flows and closure in (1.1) is only required to describe the turbulent flux of $\widetilde{c}$, $\overline{\rho u_i'' c''}$, and the mean source term, $\overline{\dot{\omega}_c}$.

1.1. *Closure models for the turbulent transport of* $\widetilde{c}$

The modelling of the turbulent flux of the mean reaction progress variable remains controversial in current combustion models. For instance, many models assume a simple gradient diffusion (GD) approximation:

$$\overline{\rho u_i'' c''} \equiv \overline{\rho}\widetilde{u_i'' c''} = -\frac{\mu_t}{\sigma_c}\frac{\partial \widetilde{c}}{\partial x_i}, \tag{1.2}$$

where μ_t is a turbulent diffusivity; and σ_c a turbulent Schmidt number. Equation (1.2) is a standard approximation used in turbulent mixing problems to describe the transport of inert species by turbulent eddies. For combustion problems, however, theoretical analysis has pointed out the existence of counter-gradient turbulent diffusion (Libby & Bray 1981; Bray *et al.* 1981). Counter-gradient diffusion (CGD) is generally related to the differential effect of pressure gradients on cold, heavy reactants and hot, light products. This effect may be shown very simply using the classical flamelet assumption of fresh reactants ($c = 0$) and fully burnt products ($c = 1$) separated by thin flame sheets. In the Bray–Moss–Libby model, this assumption translates to a bimodal probability density function for c and the turbulent flux is then expressed as (Bray 1980)

$$\overline{\rho}\widetilde{u_i'' c''} = \overline{\rho}\widetilde{c}(1 - \widetilde{c})(\overline{u_{ib}} - \overline{u_{iu}}) \tag{1.3}$$

where $\overline{u_{iu}}$ ($\overline{u_{ib}}$) is the conditional mean velocity within unburnt (burnt) gas. Let us consider a left-travelling flame along the x_i-direction ($\partial\widetilde{c}/\partial x_i > 0$). Thermal expansion and the associated flow acceleration through the flame will tend to make $\overline{u_{ib}}$ greater than $\overline{u_{iu}}$, thereby promoting counter-gradient turbulent diffusion of $\widetilde{c}$ ($\overline{\rho}\widetilde{u_i'' c''} > 0$ in

(1.3), contrary to the predictions from (1.2)). Note that counter-gradient diffusion has been observed in a number of experiments (Moss 1980; Shepherd, Moss & Bray 1982; Cheng & Shepherd 1991; Armstrong & Bray 1992). These experiments, however, correspond to rather weakly turbulent flames and the exact domain of occurrence of counter-gradient scalar transport remains unknown. Note also that in the case of counter-gradient diffusion, simple algebraic closures based on the eddy viscosity concept cannot be used and alternative proposals must be sought. One alternative proposal may be found in the Bray–Moss–Libby model where closure is achieved by writing a transport equation for $\overline{\rho u_i'' c''}$ (Bray 1980, 1990; Bray, Champion & Libby 1989).

1.2. *Closure models for the mean production of* $\widetilde{c}$

In the flamelet theory for turbulent premixed combustion, the reaction zone is assumed to be a thin surface separating fresh and burnt gases. The local, instantaneous reaction rate may be expressed in terms of the local flame surface-to-volume ratio, σ, and the ensemble-averaged reaction rate may then be expressed in terms of the mean flame surface-to-volume ratio, also called the flame surface density, $\Sigma \equiv \overline{\sigma}$ (Bray 1980; Williams 1985; Peters 1986; Trouvé & Poinsot 1994):

$$\overline{\dot{\omega}_c} = \rho_u \langle S_C \rangle_S \; \Sigma, \tag{1.4}$$

where ρ_u is the mass density in the unburnt gas; S_C is the reactant consumption speed; and $\langle \; \rangle_S$ denotes a flame surface mean defined as an area-weighted ensemble average (Pope 1988), $\langle q \rangle_S \equiv \overline{q\sigma}/\overline{\sigma} = \overline{q\sigma}/\Sigma$. The mean consumption speed, $\langle S_C \rangle_S$, accounts for local variations of the reaction rate along the flame surface while the flame surface density, Σ, characterizes the flame wrinkling due to the turbulent motions. For flames with Lewis numbers close to unity, $\langle S_C \rangle_s$ remains close to the laminar flame speed, s_L, and to first order the mean reaction rate is proportional to Σ (Haworth & Poinsot 1992; Rutland & Trouvé 1993; Trouvé & Poinsot 1994):

$$\overline{\dot{\omega}_c} = \rho_u s_L \Sigma. \tag{1.5}$$

Various model descriptions of flame surface density may be found in the literature, ranging from simple algebraic closures as proposed in the Bray–Moss–Libby approach (Bray *et al.* 1989; Bray 1990) to full transport equations as proposed in the coherent flame model (Marble & Broadwell 1977; Darabiha *et al.* 1987; Maistret *et al.* 1989; Candel *et al.* 1990). In the coherent flame model, the flame surface density is obtained via a modelled formulation of an exact evolution equation called the Σ-equation (Pope 1988; Candel & Poinsot 1990):

$$\frac{\partial \Sigma}{\partial t} + \frac{\partial \widetilde{u}_i \Sigma}{\partial x_i} + \frac{\partial \langle u_i'' \rangle_S \Sigma}{\partial x_i} + \frac{\partial \langle w n_i \rangle_S \Sigma}{\partial x_i} = \langle \kappa \rangle_S \Sigma. \tag{1.6}$$

where w is the flame front propagation speed; n_i is the flame-normal vector pointing into the unburnt gas; and κ is the turbulent flame stretch. The three convective terms on the left-hand side of (1.6) are transport terms that correspond respectively to convection by the mean flow, turbulent diffusion, and flame propagation. The term on the right-hand side of the equation is the source/sink term for flame surface density that accounts for production of flame surface area due to hydrodynamic straining and dissipation due to the combined effects of flame propagation and flame surface curvature (Trouvé & Poinsot 1994).

Different closure assumptions are required in the Σ-equation, in particular to calculate: the turbulent diffusion velocity, $\langle u_i'' \rangle_S$; the transport due to flame propagation,

$\langle wn_i \rangle_S$; and the turbulent flame stretch, $\langle \kappa \rangle_S$. We refer the reader to Duclos, Veynante & Poinsot (1993) for a critical review of the different formulations of the modelled Σ-equation that can be found in the literature. This review shows in particular that while models based on the Σ-equation differ in their description of turbulent flame stretch, these models always resort to gradient transport assumptions to close the turbulent diffusion term. Contrary to the equation for $\widetilde{c}$, the existence of counter-gradient diffusion in the Σ-equation is not considered in current combustion models. Σ and $\widetilde{c}$, however, are interrelated quantities and in case of counter-gradient diffusion of $\widetilde{c}$, gradient transport assumptions for Σ become questionable. One relation between Σ and $\widetilde{c}$ is given in (1.5) where Σ appears as a source term for $\widetilde{c}$. Another relation may be found in a theoretical study by Pope (1988) where Σ is expressed in terms of statistical properties of the c-field (one well-known piece of evidence of Σ being a function of the c-field is that Σ must vanish when the reaction reaches completion and $\widetilde{c}$ approaches unity). These theoretical ties between $\widetilde{c}$ and Σ must have some implications for the modelling of the turbulent fluxes, $\overline{\rho u_i'' c''}$ and $\langle u_i'' \rangle_S \Sigma \equiv \langle u_i'' \sigma \rangle$. These implications remain unknown.

The objective of this research is to provide basic information about turbulent transport of $\widetilde{c}$ and Σ in turbulent premixed flames. In the following, direct numerical simulation (DNS) is used to get estimates of the turbulent fluxes and study the occurrence of counter-gradient diffusion of $\widetilde{c}$ and/or Σ. Simulations from three different DNS databases are analysed in the present paper (§2). These simulations correspond to different flame–flow conditions and are compared in §3. The analysis reveals the existence of two different regimes for turbulent transport in premixed flames: a regime characterized by counter-gradient scalar transport and a regime characterized by gradient scalar transport. A simple criterion is proposed in §4 to delineate between those two regimes. A different perspective is then adopted in §5 where DNS is used to estimate the different terms appearing in the turbulent $\widetilde{c}$-flux budget. Finally, the relation between the turbulent fluxes of $\widetilde{c}$ and Σ is studied in §6.

2. Numerical simulations

Three different DNS databases are used in the present work: (i) a first database previously developed at the Center for Turbulence Research (Stanford University, USA) and referenced here as the CTR database; (ii) a second database previously developed by Professor C. J. Rutland (University of Wisconsin at Madison, USA) and referenced as the Rutland database; (iii) a third database developed in the course of this study at the Centre de Recherche en Combustion Turbulente (Ecole Centrale Paris, Institut Français du Pétrole and CERFACS, France) and referenced here as the CRCT database. Similarities and differences between the three databases are described as follows.

The simulations stored in the CTR and CRCT databases were performed using two different versions of the same DNS code originally developed at Stanford University. The Stanford code is a finite-difference solver that fully resolves the compressible Navier–Stokes equations combined with a simple but finite-rate chemistry model. The chemistry model is a single-step, irreversible, global reaction with Arrhenius kinetics. We refer the reader to Poinsot & Lele (1992), Trouvé & Poinsot (1994) and Baum (1994) for further details concerning the system of equations solved and the numerical methods. The simulations stored in the Rutland database were performed using a finite-difference/pseudo-spectral code that fully resolves the low Mach number Navier–Stokes equations combined with single-step, Arrhenius chemistry. We refer

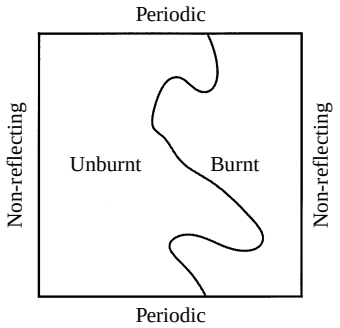

FIGURE 1. Numerical configuration.

the reader to Rutland & Cant (1994) and Zhang (1994) for further details concerning the low Mach number formulation and the numerical methods used in the Rutland code. Note that the Rutland code assumes a constant viscosity, whereas the CTR and CRCT codes feature temperature-dependent transport coefficients.

The computational configuration is similar in the three databases and corresponds to a premixed flame freely propagating into isotropic turbulent flow. The calculations are initialized with fresh reactants on the left-hand side of the domain ($x < 0$) and burnt products on the right ($x > 0$); the two are separated by a plane laminar flame. Isotropic turbulence is initially specified according to a model energy spectrum. The left- and right-hand sides of the computational domain are inflow and outflow boundaries (non-reflecting conditions), while periodic boundary conditions are applied at lateral walls (figure 1). Note that the problem is statistically one-dimensional. Mean quantities are functions of streamwise location x and time t, and can be obtained by spatial-averaging in the homogeneous (y, z)-planes. Additional information on the diagnostics used to extract statistical information from the DNS, and in particular on the methodology that is used to estimate flame surface-based quantities like Σ or $\langle u_i'' \rangle_S$, can be found in Trouvé & Poinsot (1994).

One important difference between the three databases is that in the Rutland database, turbulence is generated at the inflow boundary and the turbulent kinetic energy remains approximately constant, whereas in the CTR and CRCT databases, no turbulence is injected into the computational domain and the turbulent kinetic energy is decaying rapidly. Clearly, the analysis of the CTR and CRCT simulations is rendered difficult by the time-evolving flow and flame conditions. Unfortunately, these difficulties are only partially overcome in the Rutland database where the turbulent flow is approximately stationary but the turbulent flame, evolving from an initially flat surface to a fully wrinkled surface, is not. None of the three databases is free of initial conditions effects and comparisons with turbulent combustion models are limited to physical and qualitative observations.

Also, the simulations are three-dimensional in the CTR and Rutland databases (the grid size is respectively 128^3 and $251 \times 128 \times 128$) and two-dimensional in the CRCT database (the grid size is 257^2). Two- and three-dimensional databases represent two different compromises between completeness, accuracy and computational efficiency. While three-dimensional simulations are clearly desirable as they provide a more complete physical description of turbulent flames, their computational cost is such (typically from 50 to 100 hours of CPU time on a Cray C90) that they cannot be used for parametric studies. Hence, while the CTR and Rutland simulations capture more of the physics at play in turbulent premixed flames, they are also limited to

Case	CTR	CR	A	B	C	D
Dimension	3D	3D	2D	2D	2D	2D
τ	3	2.3	3	3	3	3
u'_0/s_L	10	1	2	3	5	10
l_{t0}/δ_L	5	30	11	11	11	11

TABLE 1. Numerical conditions. τ is the heat release factor, u'_0, the initial velocity fluctuation, s_L the laminar flame speed, l_t, the turbulent lengthscale and δ_L, the laminar flame thickness.

a single set of run parameters. In comparison, the CRCT database neglects three-dimensional dynamical effects but covers a wider range of flame–flow conditions. Table 1 displays the parameters of the six DNS runs analysed in the present work (two three-dimensional cases and four two-dimensional cases refered as A to D, with the same initial turbulence integral length scale l_t and an increasing initial turbulent r.m.s. velocity u'_0). Cases A to D are only a selection of the many runs stored in the CRCT dabase. More runs have been performed to help delineate between the counter-gradient and the gradient transport regimes. These runs are not reported in detail in the paper but they are used to validate the criterion proposed in §4 and are included in figure 17.

The flame–flow conditions in the CTR and CRCT databases are characterized by an initial turbulent r.m.s. velocity that is higher than the laminar flame speed, $u'_0/s_L = 2$–10, an integral lengthscale that is larger than the flame thickness, $l_{t0}/\delta_L = 3$–40, where δ_L is defined as the thermal diffusivity divided by the laminar flame speed, $\delta_L = D_{th}/s_L$, and a heat release factor typical of combustion situations, $\tau \equiv (T_b - T_u)/T_u = 3$–$6$, where T_u (T_b) is the temperature within unburnt (burnt) gas. The flame–flow conditions in the Rutland database are characterized by large lengthscales, $l_{t0}/\delta_L = 30$, and weak turbulence, $u'_0/s_L = 1$. Thus, the three databases correspond to different turbulent combustion regimes: highly stretched flames for the CTR database; flames with moderate to high stretch values for the CRCT database; and weakly turbulent flames for the Rutland simulations. Also, it is worth emphasizing that all simulated flames are believed to be representative of the flamelet regime. This aspect remains somewhat controversial since different criteria are availble in the literature to define the validity of the flamelet picture (Bray 1980; Williams 1985; Peters 1986; Poinsot, Veynante & Candel 1991; Roberts *et al.* 1993). For instance, the CTR simulation corresponds to flamelet combustion according to the definitions of Poinsot *et al.* (1991) and Roberts *et al.* (1993), but to non-flamelet combustion according to the classical Klimov–Williams criterion (see figure 17). In the absence of agreement between the different criteria, a careful direct examination of the flame topology was performed using three-dimensional graphics. As discussed in Trouvé & Poinsot (1994), visual inspections of the flame topology are well suited to determine whether the chemical reaction is flamelet-like and occurs on a surface (characterized by a thickness close to the laminar flame thickness δ_L) or is distributed and occurs in a volume (characterized by a size much larger than δ_L). Using this definition, we found that the simulated flames occur in the flamelet regime.

In summary, despite significant differences between the three databases (fully compressible *vs.* low Mach number simulations; stationary *vs.* decaying turbulence; three-dimensional *vs.* two-dimensional simulations), the simulated flames are all good examples of freely propagating planar turbulent flames. They correspond to different

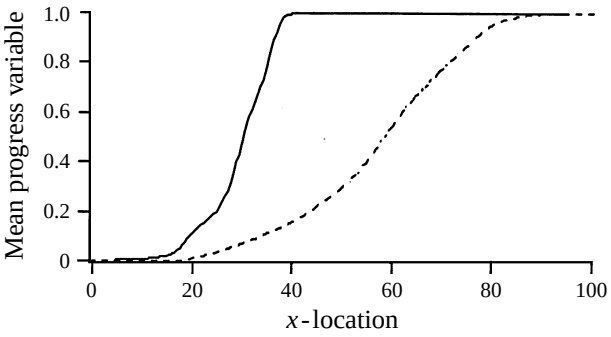

FIGURE 2. Comparison between the CTR (———) and the Rutland (– – – –) DNS. The mean reaction progress variable, $\widetilde{c}$, is plotted as a function of x-location along the direction of mean flame propagation. The comparison is performed at a time selected so that the turbulent flame speed is approximately the same in both cases. Time is $t = 4.3 l_{t0}/u'_0$ in the CTR database and $t = 4.7 l_{t0}/u'_0$ in the Rutland database. Lengthscales are made non-dimensional by the laminar flame thickness, δ_L.

turbulent combustion regimes (weak turbulence levels in the Rutland database; moderate to high turbulence levels in the CRCT database; high turbulence levels in the CTR database) and are used in the following to characterize the effect of u'/s_L (and τ) on the turbulent transport properties of $\widetilde{c}$ and Σ.

3. A DNS-based description of gradient and counter-gradient turbulent diffusion

This section presents a detailed comparison between the CTR and Rutland simulations. These simulations are three-dimensional and are well-suited to provide global (spatially averaged) information on the turbulent flame structure (§3.1) as well as local (spatially resolved) information on flow velocity and scalar gradients in the vicinity of the flame surface (§3.2). The comparison between the CTR and Rutland databases reveals striking differences in the turbulent transport properties of the simulated flames. These differences are interpreted in §3.3.

3.1. *Global structure of the turbulent flames*

While the CTR and Rutland databases feature turbulent flames with similar values of the turbulent flame speed, $S_T \approx (1.6\text{–}1.8)\ s_L$, they also correspond to turbulent flames with significantly different structure. Figures 2 and 3 give some illustrations of these differences. Figure 2 shows two instantaneous profiles of the mean reaction progress variable versus x-location in the reaction zone, as obtained in the CTR and Rutland simulations. Figure 3 presents a similar comparison for flame surface density. It is seen that the turbulent flame brush is about three times thicker in the Rutland simulation than in the CTR case. As mentioned in §2, the Rutland simulation features larger integral lengthscales and therefore larger vortices, which account for a much thicker turbulent flame. While the reaction zone is thinner in the CTR simulation, the flame front wrinkling, as measured by the magnitude of flame surface density, is also much greater. Thus, while the overall reaction rate is approximately the same, the stucture of the two simulated flames is significantly different: the Rutland flame is thick and smooth, whereas the CTR flame is thin and wrinkled.

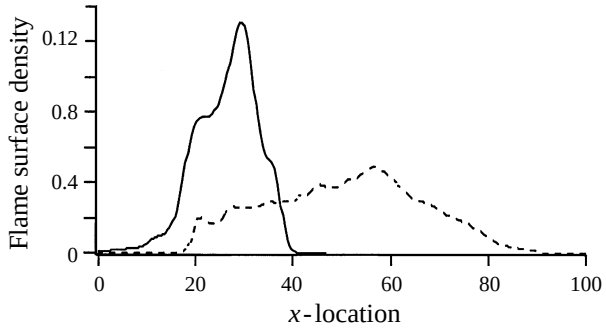

FIGURE 3. Comparison between the CTR (———) and the Rutland (– – – –) DNS. The flame surface density, Σ, is plotted as a function of x-location along the direction of mean flame propagation. Time is $t = 4.3l_{t0}/u'_0$ in the CTR database and $t = 4.7l_{t0}/u'_0$ in the Rutland database. Lengthscales are made non-dimensional by the laminar flame thickness, δ_L.

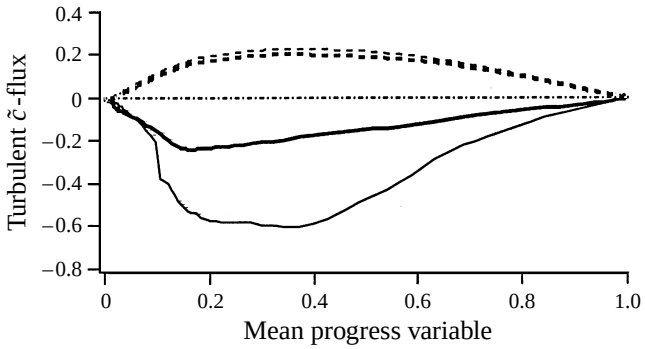

FIGURE 4. Comparison between the CTR (———) and the Rutland (– – – –) DNS. The turbulent $\widetilde{c}$-flux, $\overline{\rho u'' c''}$ (bold lines), is plotted as a function of mean reaction progress variable, $\widetilde{c}$ for time $t = 4.3l_{t0}/u'_0$ in the CTR database and $t = 4.7l_{t0}/u'_0$ in the Rutland database. In this plot, CGD (GD) corresponds to positive (negative) values of $\overline{\rho u'' c''}$. The Bray–Moss–Libby estimate, $\overline{\rho u'' c''} = \widetilde{c}(1-\widetilde{c})(\overline{u}_b - \overline{u}_u)$ (see (1.3)) is also plotted (thin lines) for comparison with the DNS data. Velocities are made non-dimensional by the laminar flame speed, s_L.

Further comparisons between the two DNS also reveal that they display striking differences in the flame turbulent transport properties. Figure 4 for instance presents typical spatial variations of the turbulent flux $\overline{\rho u'' c''}$ across the turbulent flame brush. For convenience, spatial location across the reaction zone is indicated by $\widetilde{c}$ instead of x. Figure 4 shows that the sign of the turbulent flux of $\widetilde{c}$ is different in the two DNS: the Rutland flame features counter-gradient diffusion of $\widetilde{c}$, whereas the CTR flame features gradient-like transport. Figure 5 shows that these results are consistent with the predictions from (1.3). In the Rutland simulation, the mean velocity within products, $\overline{u}_b$, is greater than the mean velocity within reactants, $\overline{u}_u$, which according to (1.3) corresponds to counter-gradient diffusion of $\widetilde{c}$. In contrast, in the CTR simulation, $\overline{u}_u$ is greater than $\overline{u}_b$, which corresponds to gradient turbulent diffusion of $\widetilde{c}$.

This last result may seem surprising since it is expected that thermal expansion will accelerate the flow field and induce a burnt-gas velocity much larger than the fresh-gas velocity. It is worth emphasizing that conditional velocities are not intuitive quantities because the sampling may be quite different for $\overline{u}_u$ and $\overline{u}_b$. For instance, at the leading edge of the turbulent flame brush (near $\widetilde{c} = 0$), the scalar

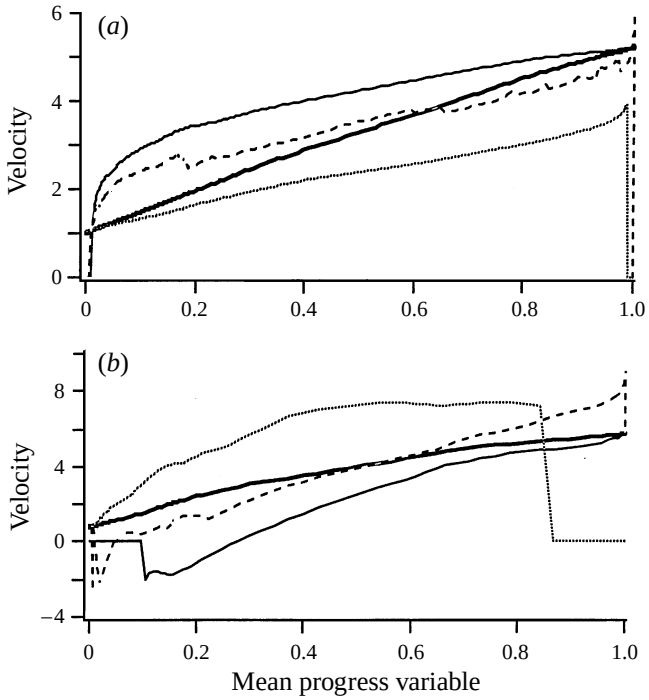

FIGURE 5. Mean flow velocities across the turbulent flame brush, as obtained: (*a*) in the Rutland database (time $t = 4.7 l_{t0}/u'_0$); (*b*) in the CTR database (time $t = 4.3 l_{t0}/u'_0$). The Favre-averaged velocity, $\widetilde{u}$ (———), the conditional mean velocities within unburnt, $\overline{u}_u$ (·····) and burnt gas, $\overline{u}_b$ (———), and the flame surface-averaged velocity, $\langle u \rangle_S$ (– – – –), are plotted in $\widetilde{c}$-space. Velocities are made non-dimensional by the laminar flame speed, s_L.

c-field corresponds mainly to instantaneous values $c = 0$, and the fresh-gas conditional velocity, $\overline{u}_u$, is computed from a large number of samples and corresponds roughly to the Favre-averaged velocity $\widetilde{u}$. At that same location, the probability of $c = 1$ is small and the burnt-gas conditional velocity, $\overline{u}_b$, is determined from a small number of samples and characterizes the motion of the flame elements lying at the leading edge. Accordingly, the slip velocity $(\overline{u}_b - \overline{u}_u)$ measures the displacement speed of the leading edge of the turbulent flame relative to the fresh gases. The same analysis may be conducted at the trailing edge of the turbulent flame ($\widetilde{c} \approx 1$). The scalar *c*-field corresponds now mainly to values $c = 1$ and the burnt-gas conditional velocity, $\overline{u}_b$, is determined from a large number of samples and is close to the mean velocity $\widetilde{u}$. On the other hand, at the same location, the fresh-gas conditional velocity, $\overline{u}_u$, is determined from a small number of samples and characterizes the motion of the flame elements lying at the trailing edge. The velocity $(\overline{u}_u - \overline{u}_b)$ becomes the displacement speed of the trailing edge of the turbulent flame relative to the burnt gases. To summarize, a positive value of the slip velocity $(\overline{u}_b - \overline{u}_u)$ corresponds to a flame brush becoming thinner and counter-gradient turbulent transport (Rutland database) whereas a negative slip velocity corresponds to a flame brush becoming thicker and gradient turbulent transport (CTR database). The discrepancy between figures 5(*a*) and 5(*b*) is one key element to understanding when gradient or counter-gradient diffusion occurs. We refer the reader to the discussion of figure 9 in §3.3 for further details.

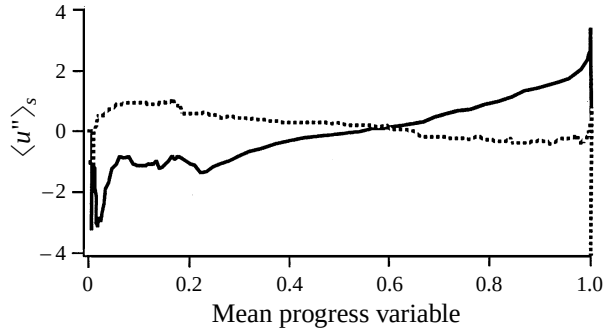

FIGURE 6. Comparison between the CTR (———) and the Rutland (– – – –) DNS. The turbulent diffusion velocity in the Σ-equation, $\langle u'' \rangle_s$, is plotted as a function of mean reaction progress variable, $\widetilde{c}$. Time is $t = 4.3 l_{t0}/u'_0$ in the CTR database and $t = 4.7 l_{t0}/u'_0$ in the Rutland database. Velocities are made non-dimensional by the laminar flame speed, s_L.

Predictions of the turbulent fluxes $\overline{\rho}\widetilde{u''c''}$ using (1.3) are also displayed in figure 4. The Bray–Moss–Libby expression (1.3) is well verified in the Rutland database but overestimates the turbulent flux by a factor of approximately 2.5 in the case of the CTR database. This discrepancy comes from the fact that, in the CTR database, the probability density function of the progress variable c is not fully bimodal. Values different from $c = 0$ or $c = 1$ should be expected as pointed out by Mantel & Bilger (1996). However, both the sign and the order of magnitude of the slip velocity, $(\overline{u}_b - \overline{u}_u)$, remain well correlated with the turbulent $\widetilde{c}$-flux, $\overline{\rho u'' c''}$, as suggested by (1.3). The non-fully bimodal p.d.f. of c leads to quantitative uncertainties but (1.3) remains a meaningful way to physically describe the turbulent transport (see §3.3).

We now turn to the turbulent transport properties for flame surface density Σ. Figure 6 presents typical spatial variations of the flow velocity fluctuation averaged along the flame surface, $\langle u'' \rangle_s$. This quantity is the turbulent diffusion velocity that appears in the Σ-equation (see (1.6)). Figure 6 shows that the variations of $\langle u'' \rangle_s$ are quite different in the two DNS: the Rutland simulation features a turbulent flux of Σ that is positive on the unburnt side of the flame and negative on the burnt side, whereas the CTR simulation features opposite trends. In the Rutland (CTR) simulation, turbulent motions occurring at the leading edge of the flame tend to push the flame surface towards burnt (fresh) gases; and turbulent motions occurring at the rear edge of the flame tend to push the flame surface towards fresh (burnt) gases. Accordingly, in the Rutland simulation, the flame thickness tends to be reduced whereas in the CTR simulation, it tends to be increased. In other words, the Rutland simulation features counter-gradient diffusion of Σ ($\langle u'' \rangle_s \Sigma / (\partial \Sigma / \partial x) > 0$), whereas the CTR simulation features gradient-like transport ($\langle u'' \rangle_s \Sigma / (\partial \Sigma / \partial x) < 0$).

3.2. *Local flow structure near the flame surface*

We now present a description of the local flow structure near the flame surface based on an analysis of the two available three-dimensional databases. The flow velocity and the c-field are spatially resolved in the DNS and can be analysed in the vicinity of the reactive layers in a frame of reference attached to the flame. This frame of reference is used in particular to determine whether local flow variations occur in directions that are normal, or tangential, to the flame surface, i.e. whether local flow acceleration vectors are aligned with, or perpendicular to, local concentration gradients of reactive species.

Note that the same frame of reference can also be used to characterize the local variations of the reaction rate, $\dot{\omega}_c$, across the flame surface. Previous studies have shown that for flames with unity Lewis numbers, the local profiles of $\dot{\omega}_c$ plotted as a function of distance along the flame normal remain approximately uniform along the flame surface (Haworth & Poinsot 1992; Rutland & Trouvé 1993). In other words, the local chemical structure of the flame remains laminar-like, a result that is consistent with the flamelet theory and shows that the chemistry of flames with unity Lewis numbers is relatively insensitive to flow perturbations. This result applies to the CTR and Rutland simulations where the local reaction rate profiles are found to be similar. The local flow velocity profiles, however, exhibit large differences, as discussed below.

Figure 7 presents typical spatial variations of flow dilatation across the flame, as obtained in the Rutland and the CTR simulations. The dilatation of the flow, $\nabla\cdot\boldsymbol{u} \equiv \partial u_i/\partial x_i$, is produced by both heat transfer in the flame preheat zone and heat release in the reaction zone. In the Rutland simulation, these local dilatation profiles are approximately uniform along the flame surface and remain laminar-like, whereas in the CTR simulation, they exhibit more variations as well as significant deviations from the laminar case.

In the Rutland simulation, the flow field is essentially one-dimensional and quasi-steady close to the flame. Most of the flame acceleration occurs along the flame-normal direction:

$$\nabla \cdot \boldsymbol{u} \approx \nabla(\boldsymbol{u}\cdot\boldsymbol{n})\cdot\boldsymbol{n}. \tag{3.1}$$

In that situation, the flow field within the flamelets is well described using classical expressions from laminar flame theory. For plane stretch-free laminar flames, the flow velocity varies linearly with c in the flame-normal direction:

$$\boldsymbol{u}\cdot\boldsymbol{n}(c) \approx \boldsymbol{u}\cdot\boldsymbol{n}(c') + \tau(c'-c)s_L, \tag{3.2}$$

$$\boldsymbol{u}\cdot\boldsymbol{t}(c) \approx \boldsymbol{u}\cdot\boldsymbol{t}(c'), \tag{3.3}$$

where $\boldsymbol{n}$ is the flame-normal unit vector pointing into the unburnt gas, $\boldsymbol{n} \equiv -\nabla c/|\nabla c|$; and $\boldsymbol{t}$ is a unit vector in the flame-tangent plane. In figure 8, (3.2) and (3.3) are re-written as

$$(\boldsymbol{u}\cdot\boldsymbol{n}(c=0.8) - \boldsymbol{u}\cdot\boldsymbol{n}(c))/\tau s_L + 0.8 \approx c, \tag{3.4}$$

$$(\boldsymbol{u}\cdot\boldsymbol{t}(c) - \boldsymbol{u}\cdot\boldsymbol{t}(c=0.8))/\tau s_L \approx 0. \tag{3.5}$$

In the Rutland simulation, these expressions are found to provide good descriptions of the local flow variations within the flamelets. In the CTR simulation, however, the flow field is not one-dimensional and cannot be deduced directly from the dilatational field. Figure 7(*b*) shows that (3.1) does not hold and figure 8(*b*) shows that the normal component of flow velocity within the flamelets does not vary linearly with c. Its gradient is not aligned with the gradient of c and it exhibits large variations from one flame location to another. Thus, while in the Rutland simulation the flow field is locally one-dimensional and fully determined by the dilatation occurring within the flame, the flow field in the CTR simulation is locally three-dimensional and dominated by the turbulent motions.

3.3. *The gradient and counter-gradient turbulent diffusion regimes*

The previous analysis suggests that the turbulent transport of $\widetilde{c}$ and Σ is determined by two different competing mechanisms (see figure 9). A first mechanism is related to thermal expansion and flame-induced motion. Thermal expansion will tend to make $\overline{u}_b$

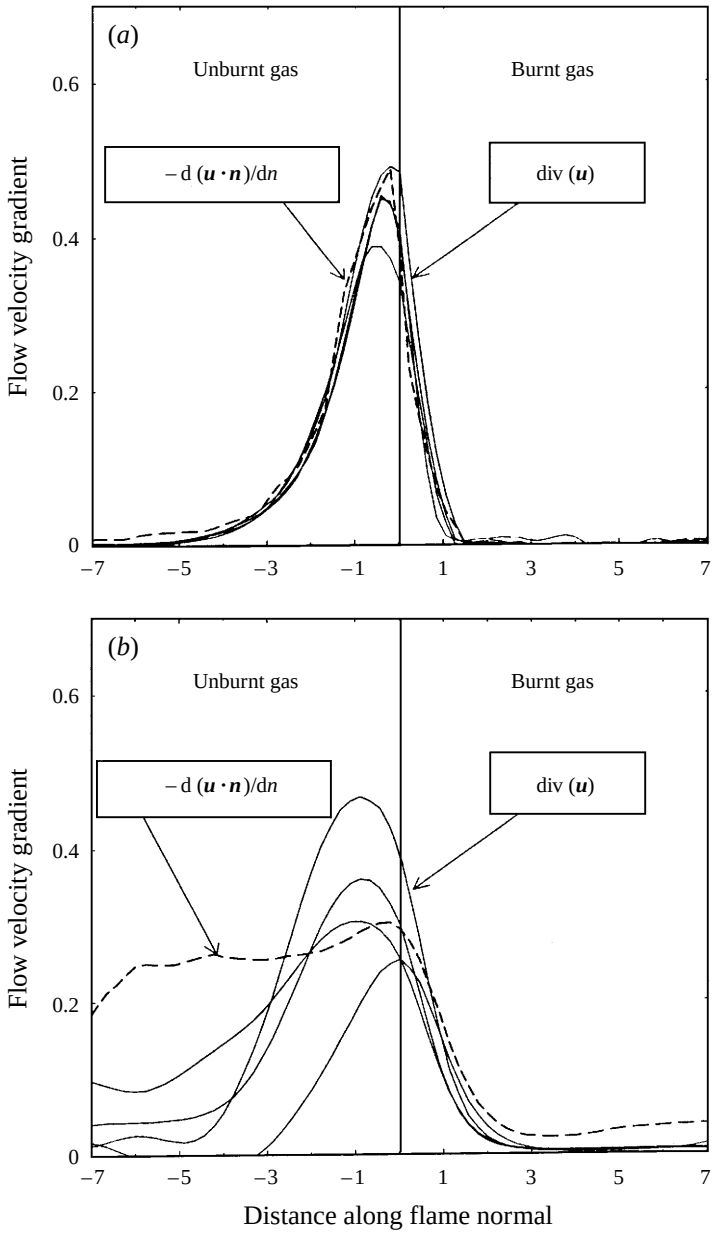

FIGURE 7. A selection of local flow dilatation profiles normal to the turbulent flame, $\nabla \cdot \boldsymbol{u}$, as a function of location along the $\boldsymbol{n}$-direction, as obtained: (*a*) in the Rutland database ($t = 4.7 l_{t0}/u'_0$); (*b*) in the CTR database ($t = 4.3 l_{t0}/u'_0$). In both figures, the dashed line is a test of the validity of equation (3.1). Quantities are made non-dimensional by the laminar flame speed, s_L, and the laminar flame thickness, δ_L.

greater than $\overline{u}_u$ and will thereby promote counter-gradient diffusion, as suggested by the classical Bray–Moss–Libby expression (1.3). This thermal expansion mechanism is to be compared to the more familiar diffusion mechanism related to the turbulent motions. At the leading edge of the flame, turbulent eddies will act to convect the flame surface towards the fresh gases. These eddies correspond to negative values of the flow

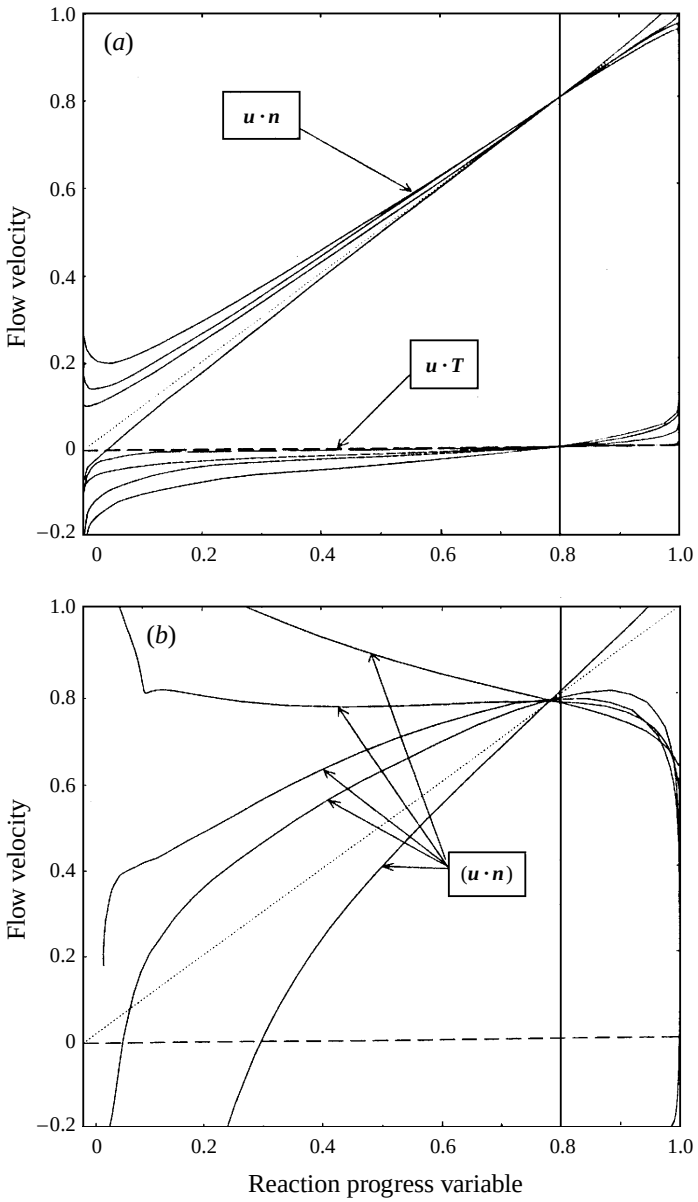

FIGURE 8. A selection of local flow velocity profiles normal to the turbulent flame, $\boldsymbol{u}\cdot\boldsymbol{n}$, as a function of location along the $\boldsymbol{n}$-direction, as obtained: (*a*) in the Rutland database ($t = 4.7l_{t0}/u'_0$); (*b*) in the CTR database ($t = 4.3l_{t0}/u'_0$). The dotted line is the curve obtained for a plane, stretch-free laminar flame (see (3.4)). In (*a*), a selection of local profiles of the tangential component of flow velocity, $\boldsymbol{u}\cdot\boldsymbol{t}$, is also shown for comparison (see (3.5)). Quantities are made non-dimensional by the laminar flame speed, s_L, and the laminar flame thickness, δ_L.

velocity fluctuation u'' and will induce negative values of $\langle u''\rangle_S$, and values of $\overline{u}_b$ lower than $\overline{u}_u$. Similarly, at the trailing edge of the flame, turbulent eddies will act to convect the flame surface towards the burnt gases. Those eddies correspond to positive values of u'' and will induce positive values of $\langle u''\rangle_S$, and values of $\overline{u}_u$ greater than $\overline{u}_b$. This turbulent transport mechanism corresponds to gradient diffusion, as suggested by (1.3).

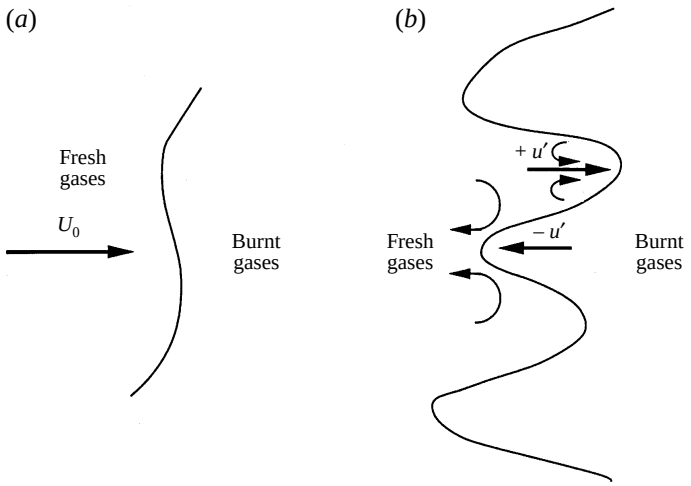

FIGURE 9. The two regimes of scalar transport: counter-gradient diffusion promoted by thermal expansion (*a*); gradient diffusion promoted by the turbulent motions (*b*).

The CTR simulation features high turbulence levels and is in fact a good example of a situation where transport of $\widetilde{c}$ and Σ is dominated by the turbulent mechanism. Gradient diffusion (GD) is then observed. In contrast, the Rutland simulation features low turbulence levels and corresponds to a situation where transport of $\widetilde{c}$ and Σ is dominated by the thermal expansion mechanism. In that situation, counter-gradient diffusion (CGD) is observed. At this point, our interpretation of the CTR and Rutland simulations suggests that GD will be promoted by high values of u'/s_L, whereas CGD will be promoted by high values of the heat release factor τ. These trends are consistent with the Bray–Moss–Libby theory (Libby & Bray 1981; Bray *et al.* 1981). Since the occurrence of GD or CGD has large implications for models, it is now important to give a more quantitative prediction of one regime or the other. In the next section, a simple model is proposed to delineate between the gradient and counter-gradient turbulent diffusion regimes.

4. Theoretical analysis

As mentioned in §2, the two three-dimensional DNS are limited by computational expense to one set of run parameters. We now resort to two-dimensional DNS to perform a parametric study of the influence of u'/s_L and τ on the flame turbulent transport properties.

Figure 10 presents the time evolution of the spatial variations of $\overline{\rho u'' c''}$ across the turbulent flame brush, for a selection of runs from the CRCT database (cases A–D in table 1). These runs only differ by the initial value of the turbulent r.m.s. velocity u'_0. Cases A–D feature an initial phase of gradient diffusion ($\overline{\rho u'' c''} < 0$). This result applies to all simulated cases and is an artifact of the initial plane flame geometry. After this initial phase, depending on the turbulence intensity, different situations are obtained. Flames interacting with weak turbulence (case A) feature CGD ($\overline{\rho u'' c''} > 0$), whereas flames interacting with strong turbulence (case D) feature GD. The CRCT database is thus capable of reproducing the two different dynamical regimes that were previously observed in the CTR and Rutland simulations.

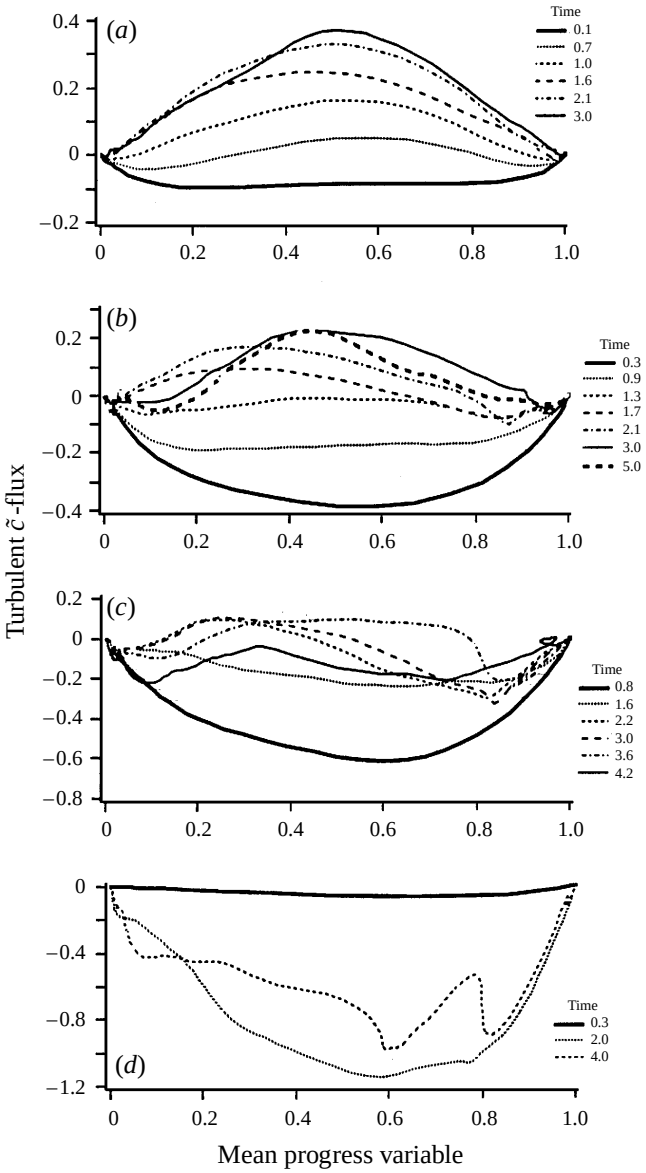

FIGURE 10. Influence of the parameter u'/s_L on flame turbulent transport properties. The turbulent $\widetilde{c}$-flux, $\overline{\rho u'' c''}$, is plotted as a function of mean reaction progress variable, $\widetilde{c}$, for a number of pre-selected times in the CRCT database. Initial velocity ratio: (*a*) case A: $u'_0/s_L = 2$; (*b*) case B: $u'_0/s_L = 3$; (*c*) case C: $u'_0/s_L = 5$; (*d*) case D: $u'_0/s_L = 10$. The heat release parameter is $\tau = 3$. Turbulent fluxes are made non-dimensional by $\rho_u s_L$ where ρ_u is the mass density of unburnt gases and s_L the laminar flame speed. Time is made non-dimensional by the initial turbulent eddy turn-over time l_{t0}/u'_0.

Similar results are also shown in figure 11 where the turbulent flux $\overline{\rho u'' c''}$ is spatially averaged over the turbulent flame brush and plotted versus time, $I(t) \equiv \int \overline{\rho u'' c''}(x,t)\mathrm{d}x$. The sign of $I(t)$ is used as a global indicator of the occurrence of GD or CGD, and provides a simple diagnostic to mark the transition from one regime to the other. Since the turbulence is time-evolving in the DNS, time in figure 11 is indicated by

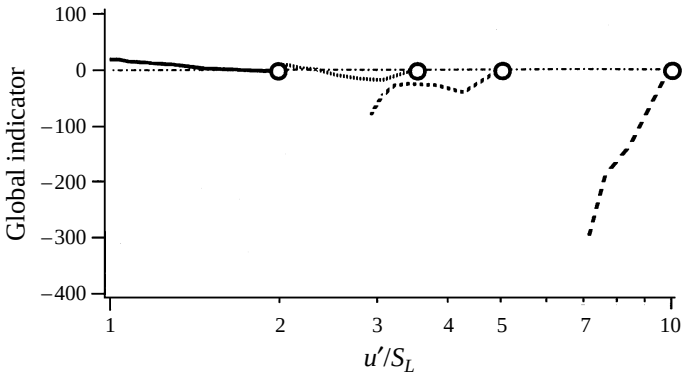

FIGURE 11. Influence of the parameter u'/s_L on flame turbulent transport properties. The global indicator, $I(t) \equiv \int \overline{\rho u'' c''}(x,t)\mathrm{d}x$, is plotted as a function of u'/s_L. $I > 0$ ($I < 0$) corresponds to CGD (GD). Each line segment corresponds to one DNS run in the CRCT database: (*a*) case A (———): $u'_0/s_L = 2$; (*b*) case B (·····): $u'_0/s_L = 3$; (*c*) case C (– – – –): $u'_0/s_L = 5$; (*d*) case D (— — —): $u'_0/s_L = 10$. Initial conditions are denoted by the symbol ○. The heat release parameter is $\tau = 3$. $I(t)$ is made non-dimensional by $\rho_u s_L \delta_L$.

u'/s_L instead of t. Flames with small values of u'/s_L ($u'/s_L < 2$) feature positive values of $I(t)$; flames with large values of u'/s_L ($u'/s_L > 7$) feature large negative values of $I(t)$; flames with intermediate values of u'/s_L ($2 < u'/s_L < 5$) feature small vanishing values of $I(t)$. Note that the intermediate zone corresponds to flame–flow conditions that are typical of many practical applications. Note also that these results are in quantitative agreement with previous results described in §3. The restriction of the CRCT simulations to two space dimensions does not seem to alter the present estimates in any significant way.

In figure 12, the turbulent flux $\widetilde{u''c''}$ in the CRCT database is compared with the Bray–Moss–Libby expression (1.3) using the fresh ($\overline{u}_u$) and burnt ($\overline{u}_b$) gas conditional velocities. As already discussed in §3.1 (figure 4), (1.3) overestimates $\widetilde{u''c''}$ because the probability density function of c is not fully bimodal in the simulations as assumed in the Bray–Moss–Libby derivation. Nevertheless, the slip velocity ($\overline{u}_b - \overline{u}_u$) is found to be strongly correlated with the turbulent flux of $\widetilde{c}$ and its sign is a good indicator of the occurrence of counter-gradient or gradient turbulent transport. Accordingly, the analysis of the slip velocity is an attractive basis for a physical description of turbulent diffusion mechanisms.

The CRCT database is now used to test a simple model developed to differentiate between GD and CGD (§4.1) and provide a criterion to predict the transition from one regime to the other (§4.2).

4.1. *A simple model for the turbulent flux of the mean reaction progress variable*

In the CTR and Rutland simulations, gradient (counter-gradient) diffusion of Σ coincides with gradient (counter-gradient) diffusion of $\widetilde{c}$. This result lends support to the idea of a possible relation between the turbulent diffusion velocity that appears in the Σ-equation (1.6) and the turbulent flux that appears in the $\widetilde{c}$-equation (1.1). This relation may be established as follows.

Following E. Bidaux & K. N. C. Bray (1994, unpublished), the flame surface-averaged flow velocity can be estimated as a weighted average of the mean unburnt

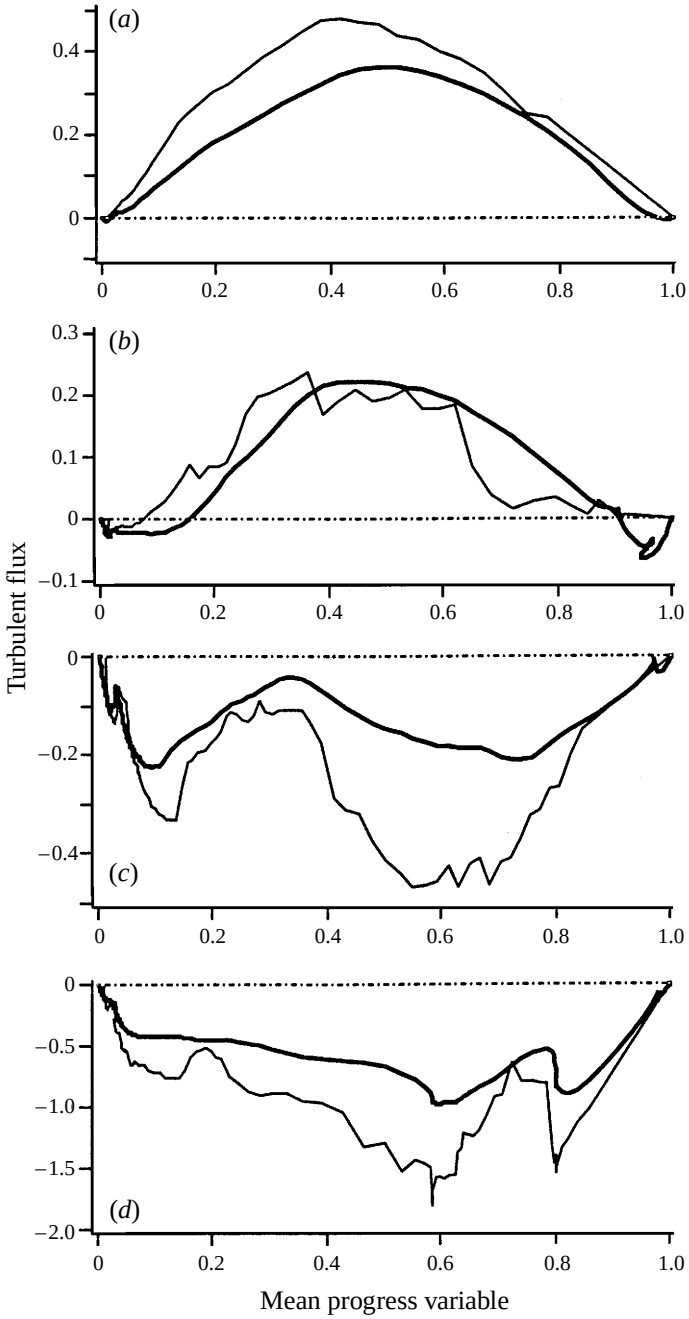

FIGURE 12. Comparison between the turbulent flux $\widetilde{u''c''}$ (bold curves) and the Bray–Moss–Libby estimate $\widetilde{c}(1-\widetilde{c})(\overline{u}_b - \overline{u}_u)$ (thin curves) for some pre-selected times in the CRCT database. Initial velocity ratio: (*a*) case A: $u'_0/s_L = 2$ ($t^+ = 3.0$); (*b*) case B: $u'_0/s_L = 3$ ($t^+ = 3.0$); (*c*) case C: $u'_0/s_L = 5$ ($t^+ = 4.2$); (*d*) case D: $u'_0/s_L = 10$ ($t^+ = 4.0$). The heat release parameter is $\tau = 3$. Time t^+ is made non-dimensional by the initial turbulent eddy turnover time l_{t0}/u'_0. Turbulent fluxes are made non-dimensional by the laminar flame speed s_L.

and burnt gases conditional velocities:

$$\langle u_i \rangle_s = (1-K)\,\overline{u_{iu}} + K\,\overline{u_{ib}} \tag{4.1}$$

where K is a constant that can be related to the iso-c line used to defined the flame location. This expression assumes a linear variation of mean flow velocity across the flame, as supported by figure 5. Furthermore, using the classical Bray–Moss–Libby framework, we can easily relate unconditional to conditional statistics:

$$\widetilde{u}_i = (1-\widetilde{c})\overline{u_{iu}} + \widetilde{c}\overline{u_{ib}}. \tag{4.2}$$

Equations (4.1) and (4.2) lead to

$$\langle u_i'' \rangle_s = \langle u_i \rangle_s - \widetilde{u} = (K-\widetilde{c})\,(\overline{u_{ib}} - \overline{u_{iu}}) \tag{4.3}$$

which, combined with (1.3), gives the final result

$$\langle u_i'' \rangle_s = \frac{(K-\widetilde{c})}{\widetilde{c}\,(1-\widetilde{c})}\widetilde{u_i''c''}. \tag{4.4}$$

Thus, the turbulent diffusion velocity, $\langle u_i'' \rangle_s$, is simply related to the turbulent flux of $\widetilde{c}$. This expression is used by Bidaux & Bray (1994, unpublished) to relate the turbulent flux of flame surface density Σ, $\langle u_i'' \rangle_s \Sigma$, to the turbulent flux of mean progress variable $\widetilde{c}$ (see equation (6.1) in §6). This expression can also be used to derive an estimate of the turbulent flux $\widetilde{u_i''c''}$ via a model for the mean velocity fluctuation $\langle u_i'' \rangle_s$. Our analysis is restricted to the present one-dimensional statistical problem and is based on the following two limiting cases pictured in figure 9.

(i) When the turbulence level is low and the flame front remains smooth, the velocity jump between fresh and burnt gases is determined primarily by thermal expansion and its value is close to that obtained in a plane laminar flame, $\overline{u}_b - \overline{u}_u \approx \tau s_L$ (Cheng & Shepherd 1991). We consider here a freely propagating turbulent flame without the additional complication of an externally imposed pressure gradient. Equation (4.3) may then be re-written as

$$\langle u'' \rangle_s = (K-\widetilde{c})\tau s_L. \tag{4.5}$$

In (4.5), the sign convention assumes that the flame travels from right ($x > 0$) to left ($x < 0$).

(ii) When the turbulence level is high and the flame front motions are controlled by the turbulent eddies, a simple estimate of $\langle u'' \rangle_s$ can be obtained by assuming linear variations in $\widetilde{c}$-space. This assumption is supported by figure 6. We write

$$\langle u'' \rangle_s = -2(K-\widetilde{c})\alpha u', \tag{4.6}$$

where u' is the turbulent r.m.s. velocity taken upstream of the flame; α is an efficiency factor to be discussed below; and where we use the following estimate: $K = 0.5$. With u' defined in the fresh gas, we implicitly assume that due to stronger viscous dissipation of turbulent eddies in the hot burnt gas, the flame front motions are dominated by the turbulence properties taken upstream of the flame. At the leading edge of the turbulent flame (near $\widetilde{c} = 0$), the flame front is convected towards the unburnt gas with a mean speed estimated by $-u'$. Similarly, at the trailing edge (near $\widetilde{c} = 1$), the flame front is convected towards the burnt gas with a mean speed estimated by $+u'$. Equation (4.6) is different from the expression proposed by Trouvé *et al.* (1994). The difference lies in the efficiency function α that has been introduced to take into account the variable ability of turbulent eddies to act on the flame front. As shown by Poinsot *et al.* (1991), small eddies are strongly affected by viscous dissipation and

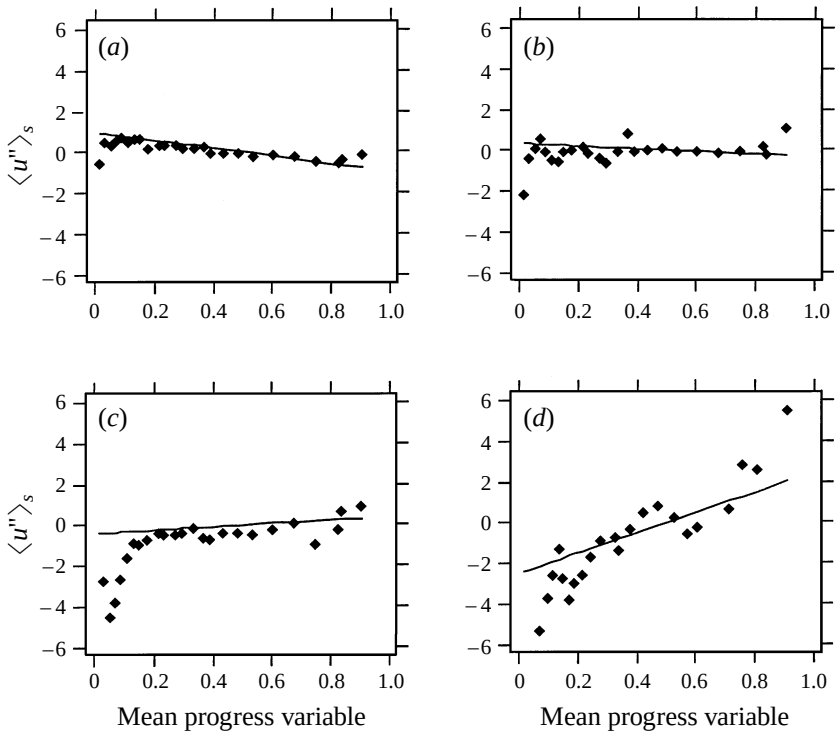

FIGURE 13. A DNS test of equation (4.7). The turbulent diffusion velocity, $\langle u'' \rangle_s$, is plotted as a function of mean reaction progress variable, $\widetilde{c}$. The solid line is the model expression (4.7) where $\alpha = 0.5$ and $K = 0.5$. The symbols are the CRCT DNS data. (*a*) Case A ($t^+ = 3.0$); (*b*) case B ($t^+ = 3.0$); (*c*) case C ($t^+ = 4.2$); (*d*) case D ($t^+ = 4.0$). Time t^+ is made non-dimensional by the initial turbulent eddy turnover time l_{t0}/u'_0. Velocities are made non-dimensional by the laminar flame speed s_L.

flame curvature effects and have a lifetime that is too short to contribute significantly to the flame wrinkling. The same phenomenon is discussed in terms of "inner cutoff scale" in a recent review paper by Gülder & Smallwood (1995). The function α has to be determined and is similar to the efficiency function introduced by Meneveau & Poinsot (1991) in their ITNFS (Intermittent Turbulent Net Flame Stretch) model. α is expected to be of order unity for large turbulent lengthscales and vanishes when turbulent eddies are too small to affect the flame front.

Combining (4.5) and (4.6), the following model is obtained:

$$\langle u'' \rangle_s = (K - \widetilde{c})\big(\tau s_L - 2\alpha u'\big) \tag{4.7}$$

which, using (4.4), gives a simple expression for the turbulent $\widetilde{c}$-flux:

$$\widetilde{u''c''} = \widetilde{c}(1 - \widetilde{c})\big(\tau s_L - 2\alpha u'\big). \tag{4.8}$$

These expressions are compared with the CRCT DNS data in figures 13 and 14, using $\alpha = 0.5$. The agreement is satisfactory: (4.7) and (4.8) are clearly capable of reproducing the transition from CGD to GD, as observed in the DNS when the ratio u'_0/s_L is increased (and keeping constant the value of the lengthscale ratio l_t/δ_L).

A first estimate of the efficiency function α is plotted in figure 15 as a function of the lengthscale ratio l_t/δ_L. This function is estimated by fitting a parabola on DNS data for $\widetilde{u''c''}$ (see (4.8)). Unfortunately, this estimate is affected by various

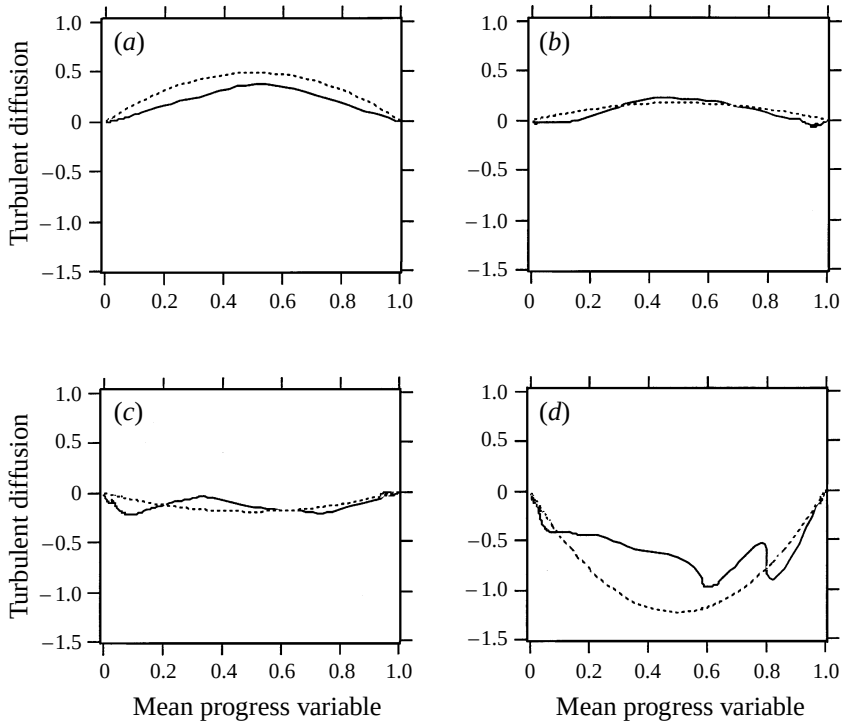

FIGURE 14. A DNS test of equation (4.8). The non-dimensionalized turbulent $\widetilde{c}$-flux, $\widetilde{u''c''}/s_L$, is plotted as a function of mean reaction progress variable, $\widetilde{c}$. The dotted line is the model expression (4.8) with $\alpha = 0.5$. The bold line is the CRCT DNS curve. (*a*) Case A ($t^+ = 3.0$); (*b*) case B ($t^+ = 3.0$); (*c*) case C ($t^+ = 4.2$); (*d*) case D ($t^+ = 4.0$). Time t^+ is made non-dimensional by the initial turbulent eddy turnover time l_{t0}/u'_0.

numerical difficulties. One major difficulty is related to the fact that the turbulence intensity u' is decaying with time. Another difficulty is the limited size of the statistical sample available in a single DNS, which accounts for the rough aspect of the different profiles extracted from the database. For intermediate values of the turbulence ratio u'/s_L, where transition between gradient and counter-gradient turbulent diffusion is observed, $\widetilde{u''c''}$ does not look like a parabola (see, for example, case C on figure 10). Most of the runs performed with different lengthscale ratios have been conducted to determin this transition region and are not well suited to determining α. Relevant information about α can only be obtained in cases that feature gradient scalar transport for a sufficiently long time. In addition, the efficiency factor α may also depend on the velocity ratio u'/s_L (as in the ITNFS function proposed by Meneveau & Poinsot 1991) and on the heat release factor τ. Further work is needed to evaluate this function in a more precise way.

The model proposed above has been derived from the CRCT database. Predictions from expressions (4.7) and (4.8) are now compared in figure 16 to the CTR and Rutland data. Even though the turbulent flux is slightly underestimated for the Rutland case and overestimated for the CTR case, the agreement is quite encouraging and the transition between gradient and counter-gradient turbulent diffusion is well predicted by (4.8).

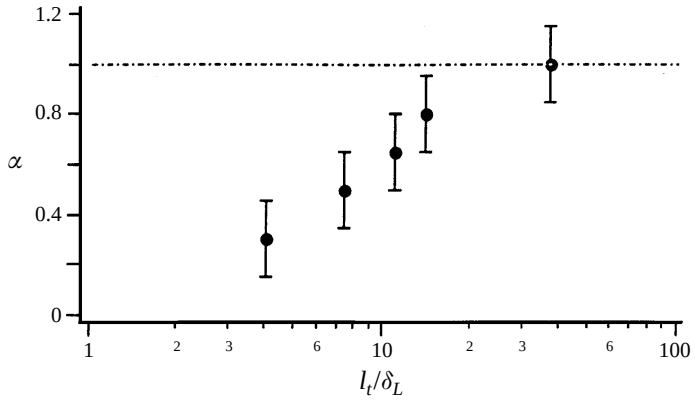

FIGURE 15. A DNS-based expression of the efficiency function α as a function of the lengthscale ratio l_t/δ_L. Numerical uncertainties are also estimated (error bars).

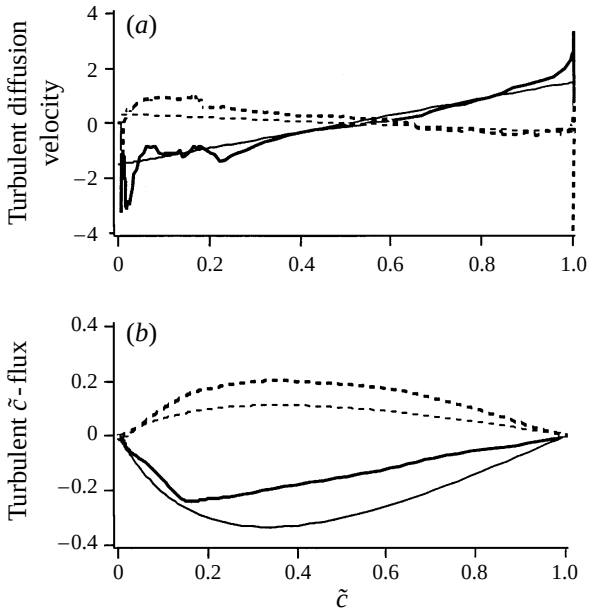

FIGURE 16. Test of equations (4.7) and (4.8) in the CTR (———) and the Rutland (– – – –) three-dimensional DNS. The turbulent diffusion velocity $\langle u'' \rangle_s$ in (*a*) and the turbulent $\widetilde{c}$-flux $\widetilde{\overline{\rho} u'' c''}$ in (*b*) are plotted as a function of the mean reaction progress variable, $\widetilde{c}$. Bold lines correspond to DNS data and thin lines to model prediction. The efficiency function α is estimated from figure 15 as $\alpha = 0.3$ for the CTR database and $\alpha = 0.8$ in the Rutland database. Time is $t = 4.3 l_{t0}/u'_0$ in the CTR database and $t = 4.7 l_{t0}/u'_0$ in the Rutland database. Velocities are made non-dimensional by the laminar flame speed s_L.

4.2. *A criterion for gradient/counter-gradient turbulent diffusion*

With our sign convention, counter-gradient diffusion corresponds to positive values of the turbulent flux $\overline{\rho u'' c''}$. From (4.8), this regime is observed when

$$\tau s_L - 2\alpha u' \geqslant 0, \tag{4.9}$$

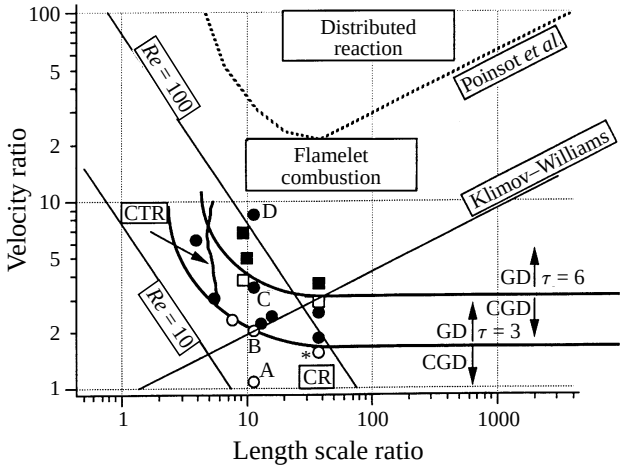

FIGURE 17. Premixed turbulent combustion diagram. The DNS flame–flow conditions are plotted as a function of the velocity ratio, u'/s_L, and lengthscale ratio, l_t/δ_L. The classical Klimov–Williams criterion and the criterion due to Poinsot *et al.* (1991) are given to show the domain of validity of flamelet combustion. Also plotted are the DNS conditions of the Rutland (CR, $\tau = 2.3$) and CTR ($\tau = 3$) simulations. As the turbulence is decaying in the CTR simulation, CTR conditions are displayed as an almost vertical line. The symbols $\circ$ ($\tau = 3$) and $\square$ ($\tau = 6$) correspond to the CRCT DNS. In two-dimensional DNS, the turbulence decay is smaller and is not represented. Filled (open) symbols denote gradient (counter-gradient) turbulent diffusion. The transition criterion, $N_B \equiv \tau s_L/2\alpha u' = 1$, separating CGD (below) from GD (above) is plotted for $\tau = 3$ and $\tau = 6$. Cases A to D are referenced whereas other data correspond to additional DNS used to determine the transition region and are not referenced in table 1.

that is when

$$N_B \equiv \frac{\tau s_L}{2\alpha u'} \geqslant 1. \tag{4.10}$$

Consistent with the Bray–Moss–Libby theory (Libby & Bray 1981; Bray *et al.* 1981), CGD (GD) is promoted by high (low) values of τs_L and low (high) values of u'. This criterion is slightly different from the one proposed by Trouvé *et al.* (1994) and its derivation is quite different. Nevertheless, it contains the same ingredients and essentially compares the strength of thermal expansion to the turbulence intensity. According to (4.10), transition from CGD to GD occurs when $N_B = 1$.

The transition criterion is plotted in figure 17 in a classical diagram for premixed turbulent combustion. The different combustion regimes are shown in this plot as a function of the turbulent-flow-to-flame lengthscale ratio, l_t/δ_L, and velocity scale ratio, u'/s_L. The domain of validity of the flamelet regime is estimated using the Klimov–Williams (KW) criterion (Williams 1985) and the Poinsot–Veynante–Candel (PVC) criterion proposed by Poinsot *et al.* (1991). As discussed in §2, PVC differs significantly from KW, particularly at small lengthscale ratios, $l_t/\delta_L < 30$. Note that the PVC criterion is supported by a recent analysis by Gülder & Smallwood (1995), where it is argued that small turbulent scales are unable to affect the flame front. The DNS data are consistent with the PVC criterion. The transition criterion, $N_B = 1$, is also plotted in figure 17, for two different values of τ, and using an estimate of α similar to the efficiency function proposed in the ITNFS model of Meneveau & Poinsot (1991). The transition criterion, $N_B = 1$, corresponds to a horizontal line at large values of l_t/δ_L. As l_t/δ_L is decreased below a value of approximately 10, the interface between CGD and GD moves upwards in the diagram due to

decreasing values of the efficiency function α. The effect of the heat release factor is straightforward: when τ is increased, GD becomes less likely and the transition line moves upwards towards higher velocity ratios. The agreement of DNS results with the criterion (4.10) is encouraging.

4.3. *Implications for gradient modelling*

In §4.2, we have proposed an algebraic expression (4.8) for the turbulent flux of $\widetilde{c}$. This expression is now compared to standard closure models based on the eddy viscosity concept. First, we use a simple estimate for the mean progress variable gradient, introducing the thickness δ_B of the turbulent flame brush:

$$\frac{\partial \widetilde{c}}{\partial x} = 4\frac{\widetilde{c}(1-\widetilde{c})}{\delta_B}, \tag{4.11}$$

where the flame brush thickness δ_B is estimated using the maximum value of the $\widetilde{c}$-gradient: $\delta_B = 1/|\partial\widetilde{c}/\partial x|_{max}$. The second term on the right-hand side of (4.8), i.e. the term that is responsible for GD, may then be re-written as

$$\widetilde{c}(1-\widetilde{c})\left(2\alpha u'\right) = \frac{\alpha}{2}\delta_B (k)^{1/2}\frac{\partial \widetilde{c}}{\partial x}, \tag{4.12}$$

where k is the turbulent kinetic energy. Note that δ_B is of the order of the integral lengthscale l_t of the turbulent flow upstream of the flame. If δ_B is interpreted as a mixing length, (4.12) is similar to the one-equation Prandtl–Kolmogorov turbulence model, and one can write

$$\widetilde{c}(1-\widetilde{c})\left(2\alpha u'\right) = \alpha\frac{\nu_t}{S_c}\frac{\partial \widetilde{c}}{\partial x}, \tag{4.13}$$

where S_c is a turbulent Schmidt number that is found to be close to 0.1 (see figure 15 in Mantel & Bilger 1996). The turbulent viscosity $\nu_t \equiv 0.5 S_c l_t (k)^{1/2}$ may be obtained, for example, from a standard $k-\varepsilon$ turbulence model. Finally, (4.8) may be rewritten as

$$\widetilde{u''c''} = \widetilde{c}(1-\widetilde{c})\tau s_L - \alpha\frac{\nu_t}{S_c}\frac{\partial \widetilde{c}}{\partial x}. \tag{4.14}$$

The second term in this expression is similar to the gradient approximation (1.2). It only differs by the introduction of an efficiency function α. The presence of α, however, clearly suggests that closure models developed in the context of turbulent non-reacting flows cannot be used directly in the case of turbulent flames. Even in the limit $N_B \to 0$, standard turbulent eddy viscosity models should be modified to account for flame surface effects.

5. Transport equation for $\overline{\rho u_i'' c''}$

A different perspective is adopted in this section where the physical phenomena responsible for the turbulent diffusion of $\widetilde{c}$ are studied using the exact transport equation for $\overline{\rho u_i'' c''}$. Bray and his coworkers (see, for example, Bray *et al.* 1981) have proposed using this equation as a basis of a closure model for the turbulent fluxes to predict the occurrence of counter-gradient turbulent diffusion. The $\widetilde{c}$-flux budget is obtained from the basic conservation equations for mass, momentum and reaction

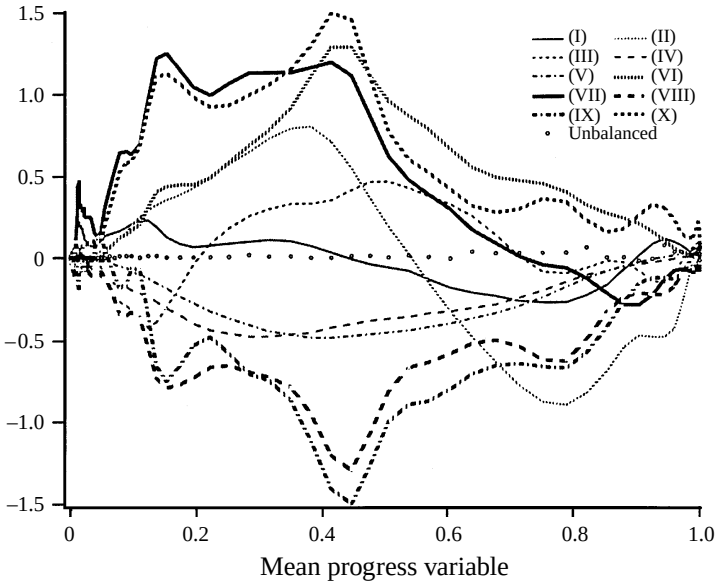

FIGURE 18. Variations of the different terms appearing in the $\widetilde{c}$-flux budget across the turbulent flame brush. Case A in the CRCT database: a case where CGD is observed (time $t = 3.0 l_{t0}/u'_0$). Quantities are made non-dimensional by $\rho_u \widetilde{u'^2_0}/l_{t0}$.

progress variable (Favre *et al.* 1976; Launder 1976):

$$\begin{aligned} \frac{\partial \overline{\rho u_i'' c''}}{\partial t} + \frac{\partial \widetilde{u}_j \overline{\rho u_i'' c''}}{\partial x_j} = &- \frac{\partial \overline{\rho u_j'' u_i'' c''}}{\partial x_j} - \overline{\rho u_j'' u_i''} \frac{\partial \widetilde{c}}{\partial x_j} - \overline{\rho u_j'' c''} \frac{\partial \widetilde{u}_i}{\partial x_j} - \overline{c''} \frac{\partial \overline{p}}{\partial x_i} \\ &\text{(I)} \quad \text{(II)} \quad \text{(III)} \quad \text{(IV)} \quad \text{(V)} \quad \text{(VI)} \\ &- \overline{c'' \frac{\partial p'}{\partial x_i}} - \overline{u_i'' \frac{\partial \mathscr{J}_k}{\partial x_k}} + \overline{c'' \frac{\partial \tau_{ik}}{\partial x_k}} + \overline{u_i'' \dot{\omega}_c}, \\ &\text{(VII)} \quad \text{(VIII)} \quad \text{(IX)} \quad \text{(X)} \end{aligned} \tag{5.1}$$

where $\mathscr{J}_k$ is the molecular diffusion flux of c; and τ_{ik} is the viscous stress tensor. In (5.1), (II) represents transport by the mean flow field, (III) transport by the turbulent flow field; (IV) and (V) are source terms due to the mean progress variable and mean velocity gradients; (VI) represents the effect of mean pressure gradients and (VII) is the fluctuating pressure term; (VIII) and (IX) are dissipation terms and (X) is the velocity–reaction rate correlation.

All terms in (5.1) can be obtained from the DNS. A typical DNS evaluation of terms (I)–(X) appearing in the $\widetilde{c}$-flux budget is presented in figure 18. The analysis serves to identify the dominant terms in (5.1) as well as the nature of their contribution. For instance, figure 18 shows that while the dissipation terms (VIII) and (IX) are of the same order and act to promote gradient diffusion, the pressure terms (VI) and (VII), and the velocity–reaction rate correlation (X), strongly act to promote counter-gradient diffusion.

Figure 18 also displays the imbalance that was found when numerically closing the $\widetilde{c}$-flux budget in (5.1). This imbalance is due to inherent numerical errors involved in the simulations as well as in the post-processing of the data. Its magnitude remains

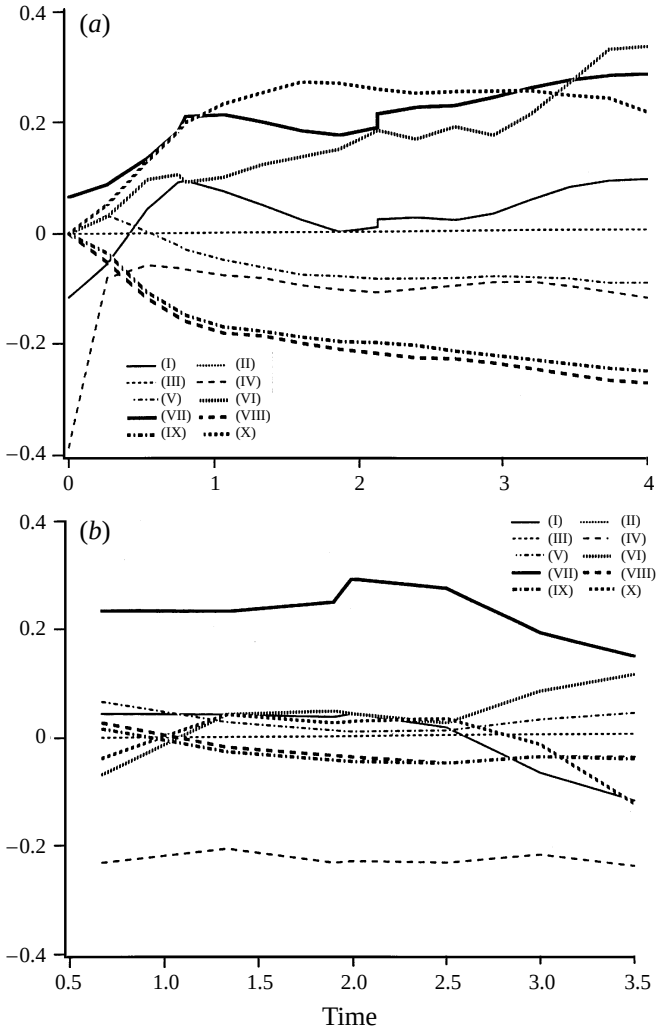

FIGURE 19. Time evolution of the different terms appearing in the $\widetilde{c}$-flux budget, after spatial-integration over the turbulent flame brush. Terms acting to promote CGD (GD) have a positive (negative) contribution in this plot. (*a*) Case A in the CRCT database ($u'_0/s_L = 2$): a case where CGD is observed. (*b*) Case C in the CRCT database ($u'_0/s_L = 5$): a case where GD is observed. The terms are made non-dimensional by $\rho_u \widetilde{u'^2_0}$. Time is made non-dimensional by the turbulent time l_{t0}/u'_0.

small, which suggests that DNS can indeed be used to analyse the variations of second-order moments.

Figure 18 corresponds to an instantaneous snapshot of the flow field. The contributions of terms (I)–(X) can also be spatially–averaged over the turbulent flame brush and plotted versus time. This provides a convenient diagnostic to visualize directly the dominant terms in (5.1). In figure 19(*a*), terms acting to promote CGD (GD) are identified by their positive (negative) contribution. Figure 19(*a*) shows that the two pressure terms (VI) and (VII), and the velocity–reaction rate correlation (X), are the main factors responsible for counter-gradient transport observed in case A. These results are consistent with the analysis by Libby & Bray (1981) which suggests

that CGD is mainly due to pressure effects. Note, however, that Bray, Moss & Libby (1982) choose to neglect the fluctuating pressure term (VII) as it is quite difficult to model. This term is found here to be of the same order of magnitude as the mean pressure term (VI) and the velocity–reaction term (X). The two dissipation terms (VIII) and (IX), which are generally modelled together, are comparable and act to promote gradient diffusion. As expected, the source term due to the mean velocity gradient (V) tends to decrease the turbulent flux and, accordingly, acts to promote gradient turbulent diffusion. The same comment applies to the source term due to the mean progress variable gradient (IV), which reduces in the present one-dimensional problem to $-\overline{\rho}\widetilde{u''^2}\partial\widetilde{c}/\partial x$. Of course, the convection (II) and diffusion (III) terms integrated over the flame brush are equal to zero.

A similar analysis is performed for case C where GD is observed (figure 19*b*). The fluctuation pressure term (VII) remains the predominant term acting to promote CGD and, once again, cannot be neglected as assumed by Bray *et al.* (1982). Nevertheless, this term fails to prevail in case C and the main factor responsible for gradient transport is the source term due to the mean gradient of the reaction progress variable (IV). As shown previously, this term is proportional to $\widetilde{u''^2}$ and its GD contribution therefore strongly increases with the turbulence intensity. The source term due to mean pressure gradient (VI) is found to have a small contribution. In this case and in the absence of an externally imposed pressure gradient, the pressure field is mainly dominated by turbulence structures and is not determined by the pressure jump at the flame front as in the previous CGD case. The flame is here unable to impose its own dynamics on the flow field. Once again, the two dissipation terms (VIII) and (IX) are comparable and promote gradient turbulent transport. As expected, the mean velocity gradient term (V) tends to decrease the turbulent flux but its contribution remains low. The velocity–reaction rate correlation (X) tends toward a strong negative contribution comparable to the unsteady term (I). The term (X) is found to have a negative contribution in case C (GD) whereas it has a positive contribution in case A (CGD). In fact, this term may be directly related to the velocity fluctuations averaged along the flame front, $\langle u''\rangle_s$. Assuming a flame surface density formulation, we can write

$$\overline{u''\dot{\omega}_c} = \overline{u''\rho_u s_L \sigma} = \rho_u s_L \langle u''\rangle_s \Sigma. \tag{5.2}$$

We now use the algebraic expression proposed by Bray *et al.* (1989) for the flame surface density Σ:

$$\Sigma \approx g\frac{\widetilde{c}(1-\widetilde{c})}{\sigma_y L_y}, \tag{5.3}$$

where σ_y is an orientation factor and L_y the flame wrinkling lengthscale. These quantities are assumed to be constant across the flame brush. g is a model constant.

Then, using (4.7) and (4.11), the integration of (X) across the flame brush leads to:

$$\int_{-\infty}^{+\infty} \overline{u''\dot{\omega}_c}dx \approx \rho_u s_L \frac{g\delta_B}{8\sigma_y L_y}(2K-1)\left(\tau s_L - 2\alpha u'\right) \tag{5.4}$$

Assuming $K > 0.5$, this term is found to be positive (negative) in the case of CGD (GD).

The classical analysis of turbulent scalar transport based on the exact $\widetilde{u''c''}$ transport equation may be directly connected to our previous approach. First, an increase of turbulence intensity tends to promote GD through the contribution (IV) of the mean

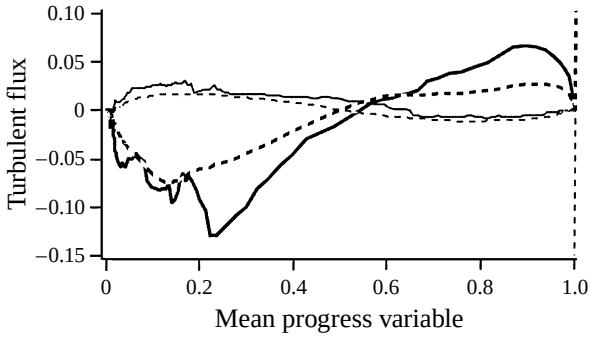

FIGURE 20. Comparison between the CTR (———) and the Rutland (———) DNS. The turbulent Σ-flux, $\langle u'' \rangle_S \Sigma$, is plotted as a function of mean reaction progress variable, $\widetilde{c}$. Dashed lines corresponds to the Bidaux & Bray estimate (6.1). Quantities are made non-dimensional by the laminar flame speed, s_L, and the laminar flame thickness, δ_L. Time is $t = 4.3 l_{t0}/u'_0$ in the CTR database and $t = 4.7 l_{t0}/u'_0$ in the Rutland database.

progress variable gradient which is directly proportional to $\widetilde{u''^2}$. The velocity–reaction rate correlation (X) is found to be representative of the turbulent diffusion regime. This term is positive for CGD and negative for GD. As shown above, this term is directly related to the mean velocity fluctuation $\langle u'' \rangle_s$. In the absence of any externally imposed pressure gradient, when the flame is able to impose its own dynamics on the flow field (Rutland case and case A), the pressure field is dominated by the pressure jump at the flame front and the mean pressure gradient term (VI), which is classically used to explain the occurrence of CGD (Bray *et al.* 1981, 1982), tends to promote CGD. On the other hand, when the turbulence intensity increases (CTR case and cases C and D), the pressure field is mainly dominated by turbulence structures, leading to a low contribution of term (VI). It is worth emphasizing that the model expression (4.8) is proposed and used in this paper as a convenient basis to describe the different physical phenomena involved in turbulent scalar transport. As shown in §4.2, (4.8) leads to a simple criterion to delineate between gradient and counter-gradient turbulent transport. However, (4.8) is not proposed as a new closure model for the turbulent $\widetilde{c}$-flux. For instance, it is not clear how pressure effects, which are known to be important, can be accounted for in simple expressions like (4.8). If (5.1) is used as the basis of a second-order closure, the DNS show that the fluctuating pressure term (VII) cannot be neglected as generally assumed in previous studies (Bray *et al.* 1982).

6. The turbulent flux of flame surface density

As discussed in §4.1, the turbulent diffusion velocity, $\langle u''_i \rangle_s$, is simply related to the turbulent flux of $\widetilde{c}$ (see (4.4)). In other words, the turbulent flux of flame surface density is simply related to the turbulent flux of mean reaction progress variable (Bidaux & Bray 1994, unpublished):

$$\langle u''_i \rangle_s \Sigma = \frac{(K - \widetilde{c})}{\widetilde{c}(1 - \widetilde{c})} \widetilde{u''_i c''} \Sigma \tag{6.1}$$

where $K \approx 0.5$. When applied to the present one-dimensional statistical problem, this relation shows that $\langle u'' \rangle_S \Sigma$ and $\widetilde{u''c''}$ have the same sign at the leading edge of the turbulent flame (near $\widetilde{c} = 0$), and opposite signs at the rear edge (near $\widetilde{c} = 1$). It is easy to see that based on (6.1), CGD (GD) for $\widetilde{c}$ implies CGD (GD) for Σ. These predictions are compared to the CTR and Rutland DNS data in figure 20. The

agreement is good. Note that since the turbulence intensities are higher in the CTR simulation than in the Rutland simulation, the magnitude of the turbulent fluxes is also found to be significantly higher.

Thus, the turbulent fluxes of $\widetilde{c}$ and Σ are strongly correlated. The obvious implication for models is that these fluxes should not be modelled independently. Equation (6.1) proposed by Bidaux & Bray is found to be reasonably accurate in the simulations and could serve as the basis of a model for the turbulent flux of Σ via a model for the turbulent flux of $\widetilde{c}$.

7. Conclusions

Two- and three-dimensional direct simulations of freely propagating premixed flames in isotropic turbulent flow are used in this paper to provide basic information on the turbulent fluxes of mean reaction progress variable, $\widetilde{c}$, and flame surface density, Σ, and to examine the occurrence of counter-gradient turbulent diffusion. The simulations correspond to various flame–flow conditions, i.e. various flow-to-flame velocity scale ratios, u'/s_L, lengthscale ratios, l_t/δ_L, and various values of the heat release factor, τ. All conditions are representative of flamelet combustion. The DNS reveal the existence of two different regimes for turbulent transport in premixed flames: a regime characterized by counter-gradient scalar transport and a regime characterized by gradient scalar transport. A detailed analysis of the local flow structure near the flame surface shows that these two regimes correspond to radically different flame–flow dynamics: counter-gradient diffusion occurs when the flow field near the flame is dominated by thermal dilatation due to chemical reaction, whereas gradient diffusion occurs when the flow field near the flame is dominated by the turbulent motions.

DNS are then used to propose a simple description of the turbulent flux of $\widetilde{c}$. This description rests on the following DNS-based results.

(i) Consistent with the Bray–Moss–Libby theory (Bray 1980), a strong correlation is found between the turbulent flux $\widetilde{u''c''}$ and the slip velocity $(\overline{u}_b - \overline{u}_u)$, where $\overline{u}_u$ $(\overline{u}_b)$ is the conditional mean velocity within unburnt (burnt) gas (1.3). This correlation holds even when the probability density function of c is not fully bimodal, and can be used to predict the occurrence of gradient or counter-gradient turbulent transport.

(ii) Consistent with the finding of Bidaux & Bray (1994, unpublished), the DNS show that the slip velocity, and therefore the turbulent flux $\widetilde{u''c''}$, is simply related to the flame surface averaged fluctuating velocity, $\langle u'' \rangle_s$.

(iii) At low turbulence levels, the fluctuating velocity $\langle u'' \rangle_s$ is determined by thermal expansion through the flame and may be estimated by τs_L. At high turbulence levels, $\langle u'' \rangle_s$ is determined by the turbulent motions and may be simply related to turbulence intensity u' via an efficiency function α that accounts for the variable ability of turbulent eddies to act on the flame front.

(iv) A simple description of $\widetilde{u''c''}$ is finally obtained by combining linearly the different contributions due to thermal expansion and turbulent eddies (4.8). This description is not proposed as a new closure model for $\widetilde{u''c''}$, but it provides a convenient basis to describe the different physical phenomena involved in turbulent scalar transport. It is used in the present paper to provide a simple criterion (4.10) to delineate between gradient and counter-gradient turbulent transport. This criterion suggests that the occurrence of one regime or the other is determined primarily by the ratio of turbulence intensity divided by the laminar flame speed, u'/s_L, and by the

flame heat release factor, τ. Consistent with the Bray–Moss–Libby theory, counter-gradient (gradient) diffusion is promoted by low (high) values of u'/s_L and high (low) values of τ.

(v) DNS also shows that these results are not restricted to the turbulent transport of $\widetilde{c}$. Similar results are found for the turbulent transport of flame surface density, Σ. The turbulent fluxes of $\widetilde{c}$ and Σ are strongly correlated in the simulated flames and a simple expression (6.1), proposed by Bidaux & Bray (1994, unpublished), that relates the turbulent flux of Σ to the turbulent flux of $\widetilde{c}$ is found to be valid. This expression shows that counter-gradient (gradient) diffusion of Σ always coincides with counter-gradient (gradient) diffusion of $\widetilde{c}$. The obvious implication for models is that these fluxes should not be modelled independently.

Equation (4.8) also provides insight into current closure descriptions used in turbulent combustion models. For instance, this expression suggests that standard closure assumptions developed in the context of turbulent non-reacting flows cannot be used directly to describe turbulent flames. Even in the case of gradient scalar transport, standard turbulent eddy viscosity models should be modified to account for flame surface effects. For instance, in (4.8), the turbulent viscosity is multiplied by an efficiency factor, α, that accounts for the variable ability of turbulent eddies to act on the flame front. A good candidate to approximate α is the ITNFS model proposed by Meneveau & Poinsot (1991).

Note that the present description of the turbulent flux of $\widetilde{c}$ is consistent with the classical Bray–Moss–Libby description based on the exact balance equation for $\widetilde{u_i'' c''}$. DNS show that the fluctuating pressure term $\overline{c''\partial p'/\partial x_i}$ that appears in the $\widetilde{u_i'' c''}$-equation cannot be neglected as generally assumed in Bray–Moss–Libby closures.

This research was initiated during the authors' visit to Stanford University as participants in the 1994 summer program of the Stanford University/NASA Ames Center for Turbulence Research (CTR). The authors acknowledge the fruitful interaction with other members of the combustion group during the summer program. In particular, we thank Professor C. J. Rutland and Dr R. S. Cant. In addition, we wish to thank Professor P. Moin, director of CTR, and Professor C. J. Rutland for providing access to their DNS databases. We also thank Dr M. Baum and Dr T. J. Poinsot for their help in developing the CRCT DNS database. The CRCT database was developed on a Cray C98 computer made available by Institut de Développement et de Ressources en Informatique Scientifique (IDRIS), France. Part of this work was performed during a sabbatical stay of D. Veynante at CERFACS and IMFT (Toulouse, France).

REFERENCES

Armstrong, N. W. H. & Bray, K. N. C. 1992 Premixed turbulent combustion flowfield measurements using PIV and LST and their application to flamelet modelling of engine combustion. *S.A.E. Meeting, Paper* 922322.

Baum, M. 1994 Etude de l'allumage et de la structure des flammes turbulentes. PhD Thesis, Ecole Centrale Paris, France.

Bray, K. N. C. 1980 Turbulent flows with premixed reactants. In *Turbulent Reacting Flows* (ed. P. A. Libby & F. A. Williams). Topics in Applied Physics, vol. 44, pp. 115–183. Springer.

Bray, K. N. C. 1990 Studies of the turbulent burning velocity. *Proc. R. Soc. Lond.* A **431**, 315–335.

Bray, K. N. C., Champion, M. & Libby, P. A. 1989 The interaction between turbulence and chemistry in premixed turbulent flames. In *Turbulent Reactive Flows* (ed. R. Borghi & S. N. B. Murthy). Lecture Notes in Engineering, vol. 40, pp. 541–563. Springer.

Bray, K. N. C., Libby, P. A., Masuya, G. & Moss, J. B. 1981 Turbulence production in premixed turbulent flames. *Combust. Sci. Tech.* **25**, 127–140.

Bray, K. N. C., Moss, J. B. & Libby, P. A. 1982 Turbulence transport in premixed turbulent flames. In *Convective Transport and Instability Phenomena* (ed. J. Zierep & H. Oertel). University of Karlsruhe, Germany.

Candel, S. M. & Poinsot, T. 1990 Flame stretch and the balance equation for the flame surface area. *Combust. Sci. Tech.* **70**, 1–15.

Candel, S. M., Veynante, D., Lacas, F., Maistret, E., Darabiha, N. & Poinsot, T. 1990 Coherent flame model: applications and recent extensions. In *Recent Advances in Combustion Modelling* (ed. B. Larrouturou). World Scientific.

Cheng, R. K. & Shepherd I. G. 1991 The influence of burner geometry on premixed turbulent flame propagation. *Combust. Flame* **85**, 7–26.

Darabiha, N., Giovangigli, V., Trouvé, A., Candel, S. M. & Esposito, E. 1987 Coherent flame description of turbulent premixed ducted flames. In *Turbulent Reactive Flows* (ed. R. Borghi & S. N. B. Murthy). Lecture Notes in Engineering, vol. 40, pp. 591–637. Springer.

Duclos, J. M., Veynante, D. & Poinsot, T. 1993 A comparison of flamelet models for premixed turbulent combustion. *Combust. Flame* **95**, 101–117.

Favre A., Kovasnay, L. S. G., Dumas, R., Gaviglio, J. & Coantic, M. 1976 *La Turbulence en Mécanique des Fluides*. Gauthier Villars.

Gülder, O. L. & Smallwood, G. J. 1995 Inner cutoff scale of flame surface wrinkling in turbulent premixed flame *Combust. Flame* **103**, 107–114.

Haworth, D. C. & Poinsot, T. 1992 Numerical simulations of Lewis number effects in turbulent premixed flames. *J. Fluid Mech.* **244**, 405–436.

Launder, B. E. 1976 *Heat and Mass Transport by Turbulence*. Topics in Applied Physics, vol. 12. Springer.

Libby, P. A. & Bray, K. N. C. 1981 Countergradient diffusion in premixed turbulent flames. *AIAA J.* **19**, 205–213.

Maistret, E., Darabiha, N., Poinsot, T., Veynante, D., Lacas, F., Candel, S. M. & Esposito, E. 1989 Recent developments in the coherent flamelet description of turbulent combustion. In *Proc. 3rd Intl SIAM Conf. on Numerical Combustion.*

Mantel, T. & Bilger, R. W. 1996 Some conditional statistics in a turbulent premixed flame derived from direct numerical simulation. *Combust. Sci. Tech.* **110–111**, 393.

Marble, F. E. & Broadwell, J. E. 1977 The coherent flame model for turbulent chemical reactions. *Project Squid Tech. Rep.* TRW-9-PU.

Meneveau, C. & Poinsot, T. 1991 Stretching and quenching of flamelets in premixed turbulent combustion. *Combust. Flame* **86**, 311–332.

Moss, J. B. 1980 Simultaneous measurements of concentration and velocity in an open premixed turbulent flame. *Combust. Sci. Tech.* **22**, 119–129.

Peters, N. 1986 Laminar flamelet concepts in turbulent combustion. In *Twenty-First Symp. (Intl) on Combustion*, pp. 1231–1250. The Combustion Institute.

Poinsot, T. & Lele, S. K. 1992 Boundary conditions for direct simulations of compressible viscous flows. *J. Comput. Phys.* **101**, 104–129.

Poinsot, T., Veynante, D. & Candel, S. M. 1991 Quenching processes and premixed turbulent combustion diagrams. *J. Fluid Mech.* **228**, 561–605.

Pope, S. B. 1988 Evolution of surfaces in turbulence. *Intl J. Engng Sci.* **26**, 445–469.

Roberts, W. L., Driscoll, J. F., Drake, M. C. & Goss, L. P. 1993 Images of the quenching of a flame by a vortex: to quantify regimes of turbulent combustion. *Combust. Flame* **94**, 58–69.

Rutland, C. J. & Cant, R. S. 1994 Turbulent transport in premixed flames. In *Proc. Summer Program* Center for Turbulence Research, NASA Ames/Stanford University.

Rutland, C. J. & Trouvé, A. 1993 Direct simulations of premixed turbulent flames with non-unity Lewis numbers. *Combust. Flame* **94**, 41–57.

Shepherd, I. G., Moss, J. B. & Bray, K. N. C. 1982 Turbulent transport in a confined premixed flame. In *Nineteenth Symp. (Intl) on Combustion*, pp. 423–431. The Combustion Institute.

Trouvé, A. & Poinsot, T. 1994 The evolution equation for the flame surface density in turbulent premixed combustion. *J. Fluid Mech.* **278**, 1–31.

Trouvé, A., Veynante, D., Bray, K. N. C. & Mantel, T. 1994 The coupling between flame surface

dynamics and species mass conservation in premixed turbulent combustion. In *Proc. Summer Program*. Center for Turbulence Research, NASA Ames/Stanford University.

Vervisch, L., Kollmann, W., Bray, K. N. C. & Mantel, T. 1994 Pdf modeling for premixed turbulent combustion based on the properties of iso-concentration surfaces. In *Proc. Summer Program*, Center for Turbulence Research, NASA Ames/Stanford University.

Williams, F. A. 1985 *Combustion Theory*, 2nd edn. Benjamin Cummings.

Zhang, S. 1994 Simulations of premixed flames with heat release. PhD Thesis, University of Wisconsin, Madison, USA.